Chapter 3 Diffraction

Peter Eschbach

The first thing we need to understand in discussing diffraction is plane geometry. A plane is defined by the equation,

Ax + By +Cz = D, where A, B, C, D = constant.

The trivial case is found by setting z = 0 and then the x-y plane is defined. A trick of solid geometry is to express this general equation in an intercept form by first setting y,z = 0,

Ax = D or A = $\frac{D}{x0}$.

Similarly setting x,y = 0

Cz = D or C = D/z0.

Finally, set x.z = 0,

By = D or B = D/y0.

We now have for our equation of plane,

$\frac{D}{x0}$x + $\frac{D}{y0}$y + $\frac{D}{y0}$y = D.

Dividing both sides by D,

$\frac{x}{x0}$ + $\frac{y}{y0}$ + $\frac{z}{z0}$ = 1. (3.1) We have derived a general equation for a plane now in intercept form. Notice that this equation could be the result of two perpendicular vectors one with dimensions of length the other with dimensions of $\frac{1}{length}$. It is not by accident we chose this form for the equation of a plane as it motivates what follows, a discussion of reciprocal lattice. A picture of an important plane in crystalline material is shown below and it is labelled in terms of its intercepts, 1, 1, 1.
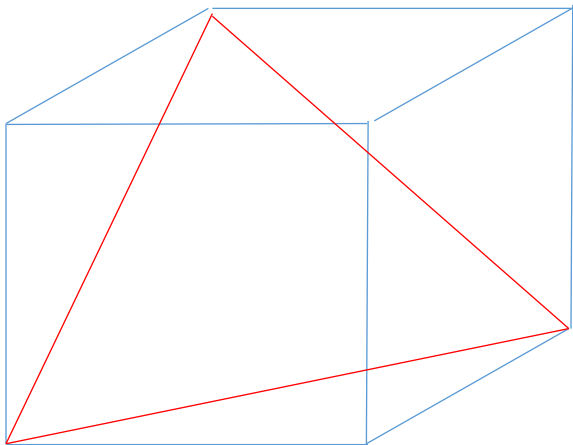

Figure 3.1 The plane expressed by intercepts 1,1,1.

The language of diffraction is in terms of these intercepts. And one convention for intercepts are Miller indices. Miller indices of a lattice plane are the coordinates of the shortest reciprocal lattice vector normal to that plane.[1] The shortest reciprocal lattice vector is a key element because it insures that there are no common factors in the Miller indices, for example, (024) is not a set of Miller indices but (012) is. Why do we express things in terms of the reciprocal lattice, besides the fact that we know equation 3.1 motivates this already? All diffraction patterns have distances between the bright spots that are inversely proportional to the lattice spacing. In other words, the reciprocal lattice points are identical to diffraction spots, with the exception of the selection rules. Therefore, reciprocal distances are the natural language of diffraction. This will be more obvious as we work through this chapter and read further. In terms of cross products, if you are familiar with those, the reciprocal lattice vectors are given by:

$a1* = \frac{a2^{\wedge}a3}{a1 \cdot a2^{\wedge}a3}$, $a2* = \frac{a3^{\wedge}a1}{a2 \cdot a3^{\wedge}a1}$, and $a3* = \frac{a1^{\wedge}a2}{a3 \cdot a1^{\wedge}a2}$ (3.2), where a1, a2 and a3 are the real space unit cell vectors. Notice that equation 3.2 has dimensions of 1/length as motivated by our plane equation, 31.

An alternate definition of reciprocal lattice is to stick with the real lattice and this may be an easier way to go for the students not so familiar with a reciprocal lattice, yet! In the real lattice definition the Miller indices are simply the inverse of all three intercepts of real space coordinates with common factors removed. So, for example if our plane of interest intercepts the x axis at 1, y axis at 1, and z axis also at 1 the miller indices are simply

$(\frac{1}{x_i}, \frac{1}{y_i}, \frac{1}{z_i}) = (\frac{1}{1}, \frac{1}{1}, \frac{1}{1})$. = (111). Where x_i is the x intercept, y_i is the y intercept and z_i is the z intercept.

Now let's consider a slightly harder case such as fractional intercepts like x_i, y_i of ½ with Z intercept of 2/3. In that case, we refer back to the definition one as the Miller indices are reciprocal lattice vector and as such, they must be integers. So by using the one over the intercept technique we have

$(\frac{1}{x_i}, \frac{1}{y_i}, \frac{1}{z_i}) = (\frac{1}{1/2}, \frac{1}{1/2}, \frac{1}{2/3}) = (2, 2, \frac{3}{2})$. Now making integer to lowest common factor we have, (4,4,3).

We can of course have negative intercepts and see them all of the time in diffraction problems, they are denoted with a negative or a bar over the number

(1,-1,1) = (1,**1**,1) where boldface 1 is -1. Graphical constructions of some of these examples appears below in figure 3.2

---

[1] "Solid State Physics," Ashcroft and Mermin, Saunders College, 1976, pp 91-92.
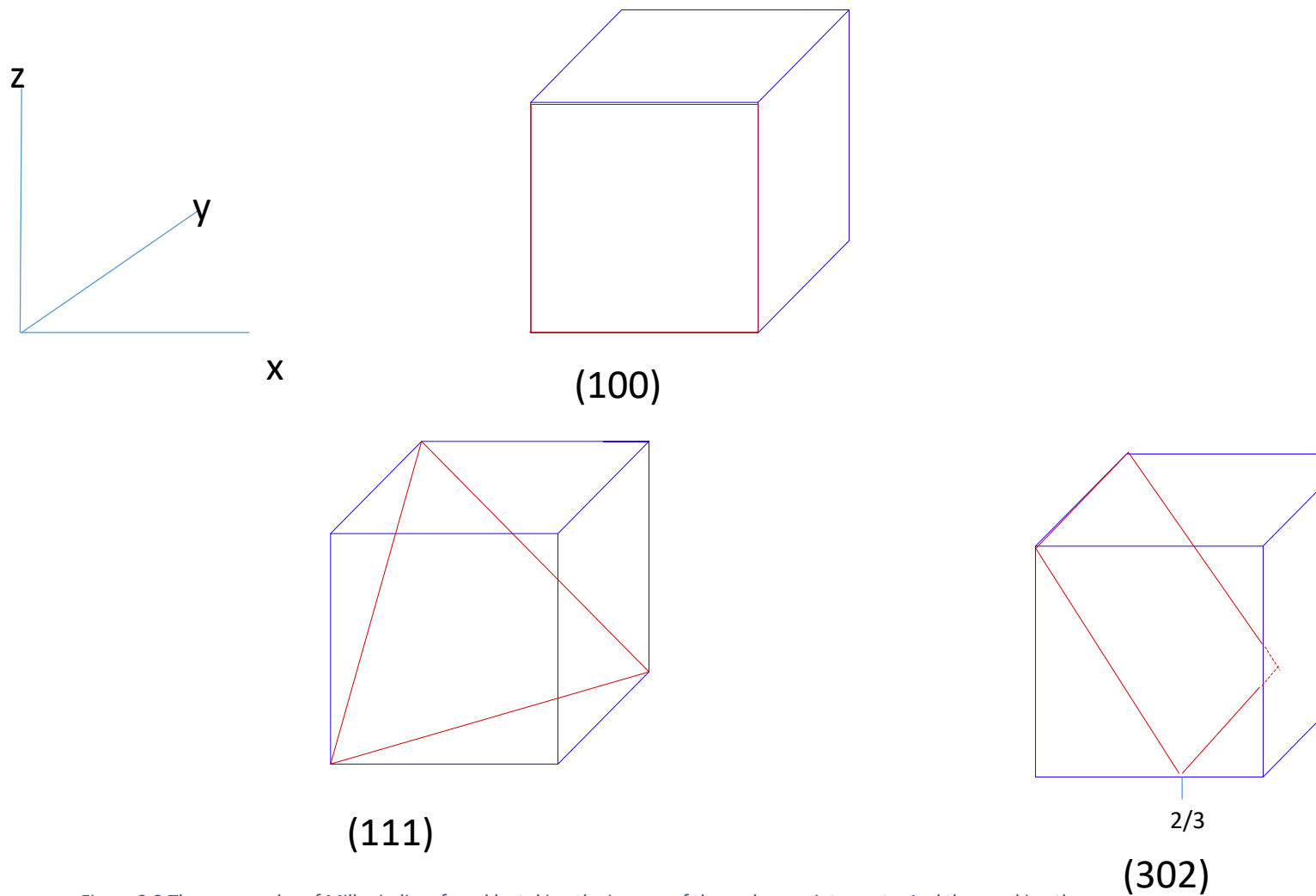
Figure 3.2 Three examples of Miller indices found by taking the inverse of the real space intercepts. And then making them integer as reciprocal lattice vectors are integers.

We have been talking about cubic systems so far. In cubic systems the reciprocal lattice vector, a_1^* is parallel to the real space lattice vector a_1. And similarly a_2^*, and a_3^* are parallel to a_2 and a_3. We can see this is the case for a cubic system from equation 3.1 above as a_1^* is in the direction $a_2 \wedge a_3$ and this is simply the x axis or a_1, see figure 3.2 below.
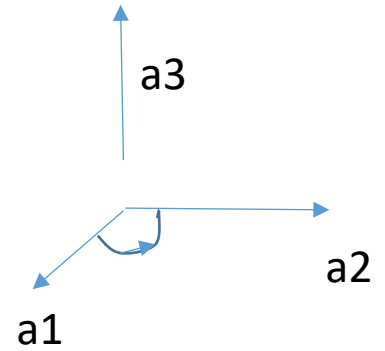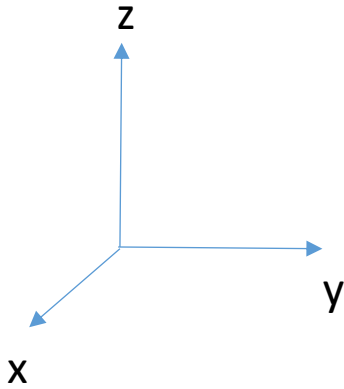
z

y

x

a3

a2

a1

Figure 3.3 The cross product of a1 and a2 is just the a3 vector parallel to the Z axis. So, in cubic systems, the reciprocal lattice vector a3* is parallel to the a3 real space unit cell vector.

This is always the case in cubic systems. However, in Hexagonal, Triclinic or Monoclinic where the angles are not all ninety degrees the reciprocal lattice vector is not parallel to the real lattice vector. Thus, in a cubic system the Miller indices of the plane normal are the same as the indices of the plane or <110> in a cubic system is perpendicular to the (110) plane. We examine the Triclinic vs the Cubic system in figure 3.4 below.

Cubic crystal

Triclinic crystal

a_3 and a_3*

a_3*

a_2

a_3

a_1

Cubic, a_1^a2 = a_3.
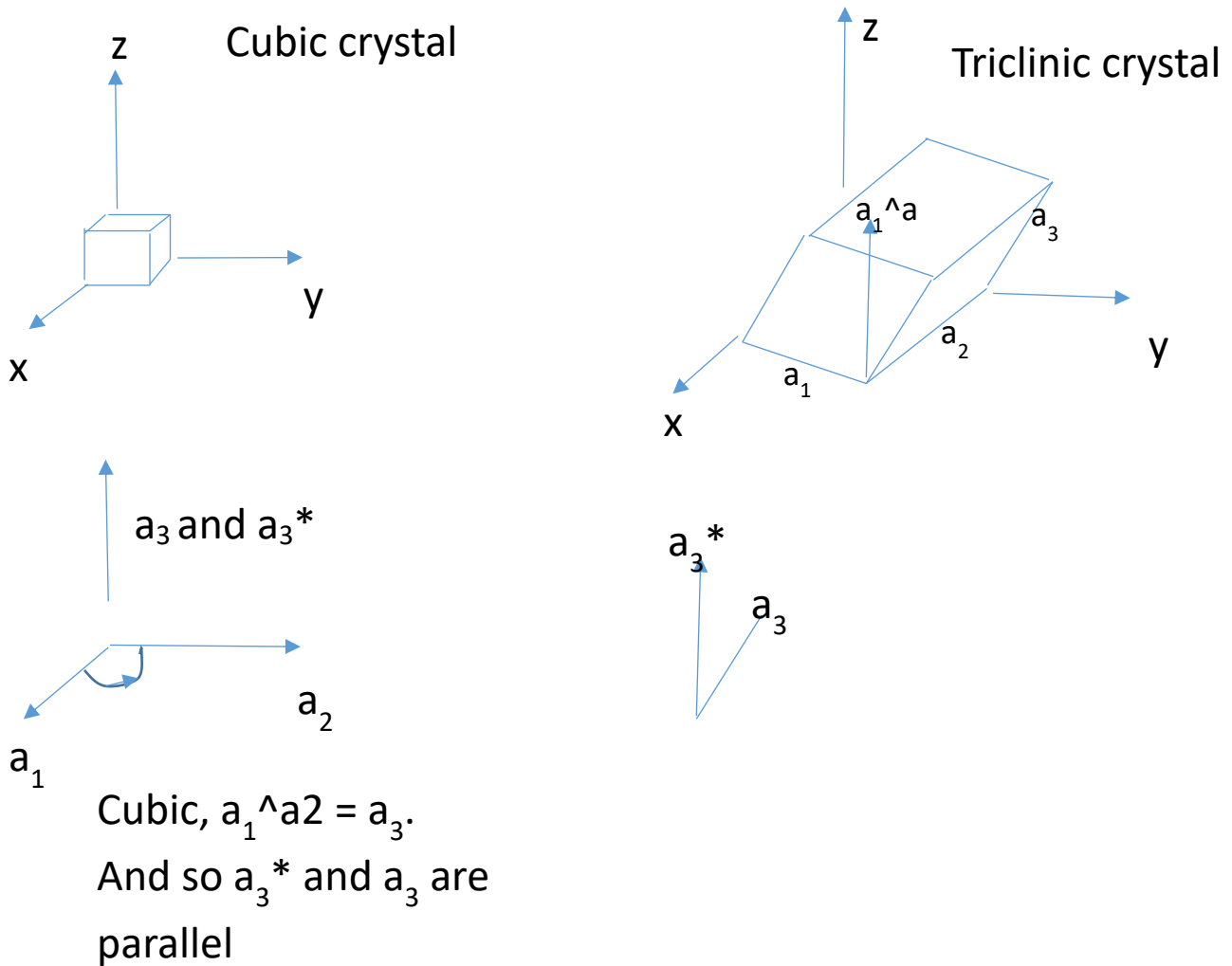And so a_3* and a_3 are parallel

Figure 3.4 Cubic and non-cubic lattices and corresponding reciprocal lattice directions. We must take care as reciprocal lattice vectors in the Triclinic system are not parallel to the regular unit cell directions.

In Figure 3.3 we speak of the caution we must have in a Triclinic system when we think of Miller indices and in general we have to take the same caution with plane normals in non-cubic systems as the plane normal is not simply given by the Miller indices of the plane in the non- cubic system. Similarly, interplanar distances are much harder to compute for non-cubic systems. Here is the expression for interplanar spacing in cubic systems:

$D_{hkl} = \frac{a}{\sqrt{h^2+k^2\ l^2}}$. Where D is the interplanar spacing and a is the lattice constant, 5.43 Angstrom for Silicon. And h,k,l are the Miller indices discussed above. We can see right away that our formalism using the intercept form to describe the plane, of equations 3.1 and 3.2 has resulted in a nice simple

expression. For Silicon, h = k = l = 1, results in the well known spacing observed over and over in TEM, 3.14 Angstrom for the (111) Silicon planes. A number that as a TEM person you will use many times.

What causes diffraction? To physicists it is a split in electron wave function as the electron approaches a boundary (first Brillouin zone). This split is manifest in the frequency vs wavenumber, w(k), relationship at the first Brillouin zone (reciprocal lattice surface) in the material. This split is where Bragg scattering occurs and physically it is where the electron wave undergoes a standing wave phenomenon in the crystal. This general diffraction criteria is equivalent to the Laue condition, k-k' = G where G is a lattice vector. This is shown below in figure 3.5 where the radius of the Ewald sphere is smaller than reality for the very short wavelength (long k) electron wave. The construction is discussed in Kittel[2]
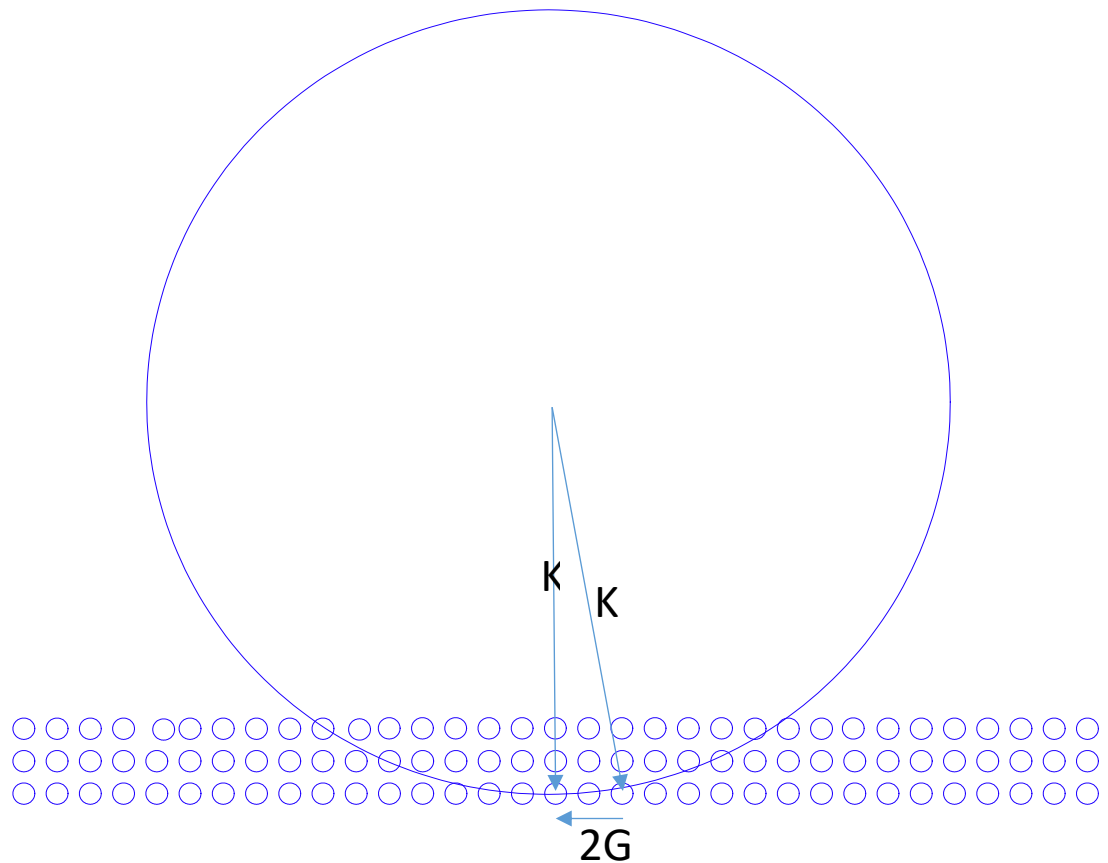

Figure 3.5 Ewald sphere construction showing that when the scattered electron wave and incident electron wave touch two lattice points a diffraction is expected. As discussed in Kittel, this occurrence is a happy accident. A second order diffraction, 2G, is shown.

---

[2] Kittel , Introduction to Solid State Physics, page 37 Wiley , 1986

In Figure 3.5 the points are reciprocal lattice points not real lattice points. The reciprocal lattice discussed later in the chapter but for now realize that the reciprocal lattice has distances of one over length and is a more convenient, mathematical construction used in diffraction. The construction of Figure 3.5 is a three dimensional theorem that holds true in general. We now talk about the two dimensional situation of Bragg's law.

Bragg's law is probably more familiar to undergraduates and we now derive it from the more general Laue condition above.
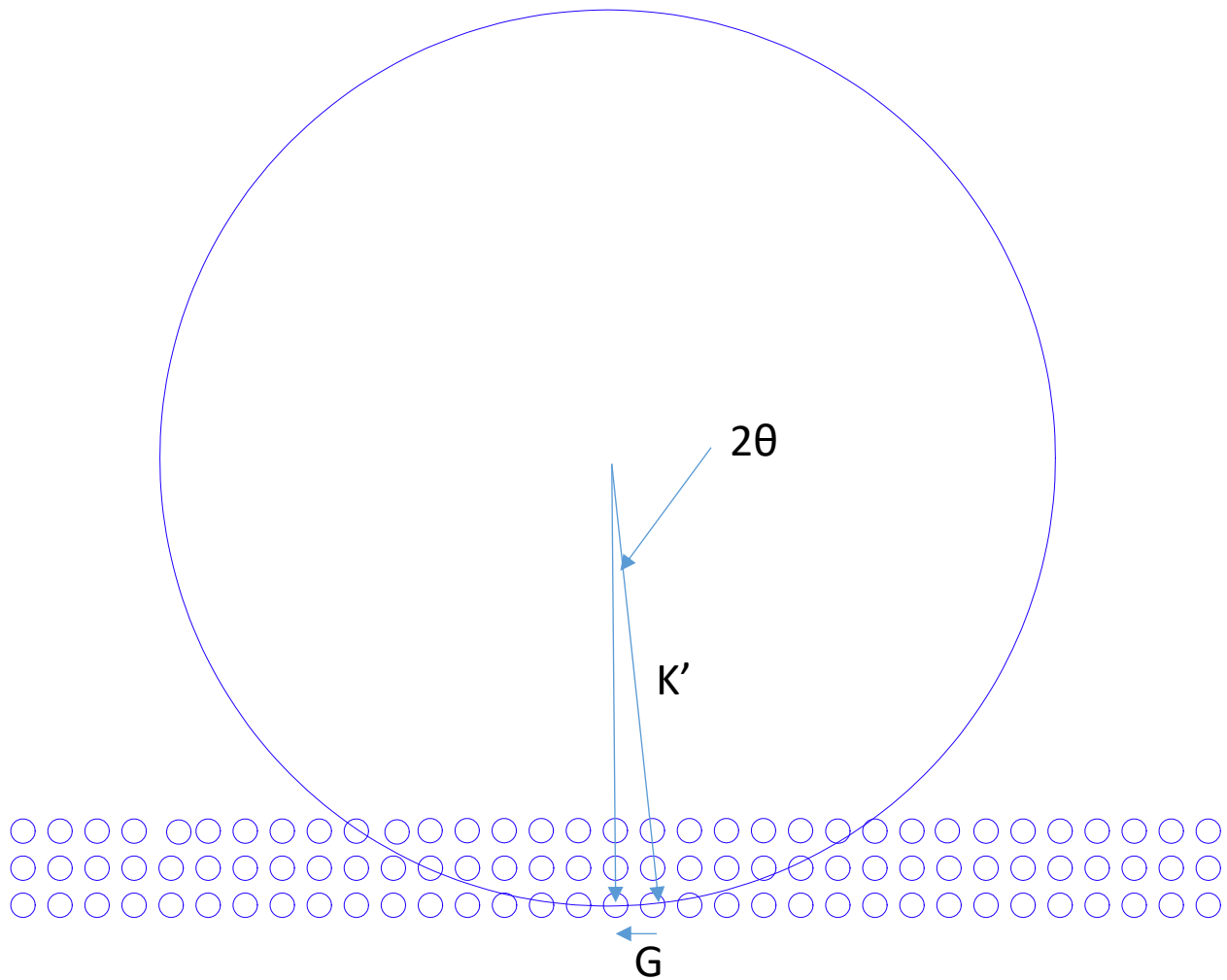

Figure 3.6 Ewald Sphere and Laue condition as a starting point for Bragg's law derivation. Note, it is important to realize that the scattering angle is not the Bragg angle. The scattering angle is 2x the Bragg angle.

From the figure,

Tan(2θ) = G/k. And now consider that k = k', elastic scattering and theta is small. We have,

Tan(2θ) ~ 2θ. And 2θ = G/k. k = $\frac{2\pi}{\lambda}$. And G = $\frac{2\pi}{d}$, where d is the lattice spacing. So now, we have,

2θ = $\frac{\lambda}{d}$. Or $\lambda = 2d\theta$. A more general derivation takes sin(θ) = $\frac{G}{2}$/|k'|. And since |k'| = |k|,

$2\mathrm{Sin}(\theta) = \frac{\lambda}{d}$. And so,

$\lambda = 2d\mathrm{sin}\theta$. This is the recognizable Bragg's law for n = 1. A more general derivation takes into account higher order reflections such as 2G, 3G, 4G, … and this is discussed in Carter and Williams. [3] These higher order reflections are due to the large diameter of the Ewald Sphere for a TEM. In X-ray diffraction the Ewald Sphere is much smaller diameter and we are much less likely to see the 2G, 3G diffractions. It was mentioned that the scattering angle is not the Bragg angle but twice. A funny story on that, in teaching a class I was locating several zone axis of Silicon. I took the dot product of the two zone axis (directions in crystal) to determine the angle between them and came up with 46 degrees. But, in tilting the sample in the TEM I soon discovered the second zone axis at a tilt of 23 degrees or half the expected value. What happened? Let's examine that situation with figure 3.3 below.
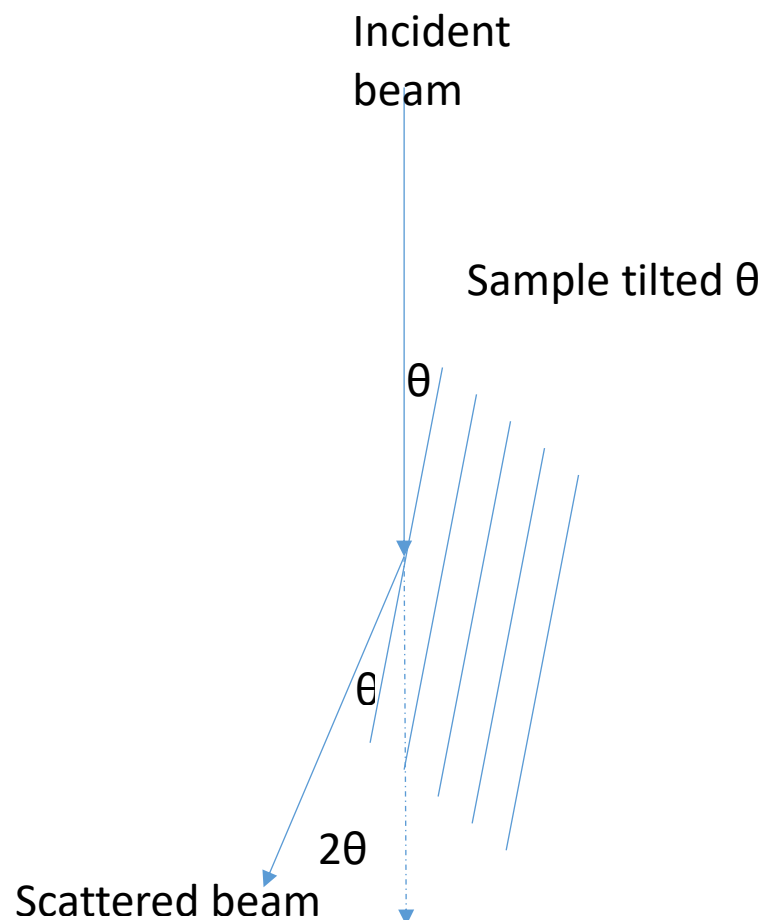

Figure 3.7 With scattered beam exiting at the incident angle, kinematic condition, the total scattered angle is 2x larger than the incident.

From Figure 3.7 the total scattered angle is two times the original angle between the planes and the incident beam. Therefore, when we tilt in the TEM we have to keep this in mind we are actually tilting two times faster than we might have thought. Fortunately, this is the case as most TEM double tilt

---

[3] Transmission Electron Microscopy, D.B. Williams and C.B. Carter, Plenum Press, pp 181-184, volume 1, 1996

holders only allow up to 30 degrees of tilt in the Beta direction thus allowing us to access up to 60 degrees separation between zone axes.

Now that we are on the topic of Ewald Spheres lets finish up with discussion of higher order Laue Zones. In one atom thick TEM sample or ones that are nearly this thin, higher order Laue Zones are not observed. This dispels the notion that thinner is always better in a TEM sample. For if we have a thicker sample we can get 3-D information and unit cell dimensions from the first and second order Laue Zones. Consider figure 3.8 below,
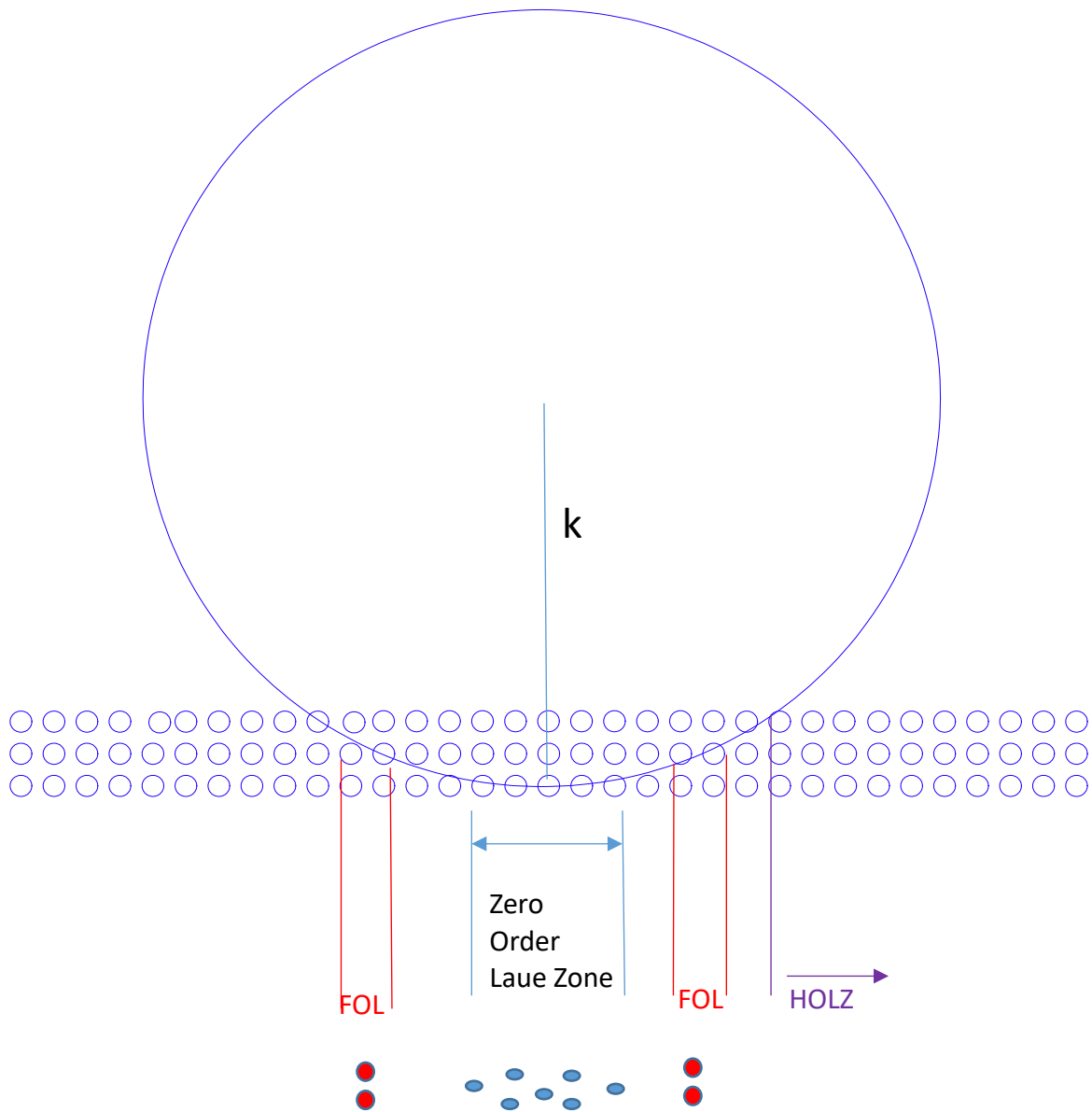
Figure 3.8 Ewald sphere construction-showing contributions from a thicker sample. These contributions from row 2 in red , row 3, are called higher order Laue zones.

In figure 3.8 the contributions are color coded light blue disks originate from the zero order Laue Zone. The red diffraction disks will actually form a ring and this ring diameter can be used to calculate the unit cell dimension parallel to the beam direction, a method we will discuss later. In addition, there are higher order Laue zones (HOLZ) as well.   The higher order is not to be confused with the 2g, 3g reflections we observed in figure 3.2. In the higher order Laue Zones the Weis' s zone law which we will discuss later is no longer zero but an integer, or the generalized Weis's zone law: uh + vk + wl = 0, 1, 2, 3, … where the integer is the order of the Laue zone. For example in Silicon a simple expression for the

<111> zone axis is derived from Weis's zero order zone law, uh +vk +wl = 0 and since uvw are all 1, we have

h + k + l = 0 for observed diffraction spots in a Si <111> pattern. If we then have shot our diffraction pattern with a short camera length and so have captured higher order Laue Zones we would have for the first order zone diffractions[4],

h + k +l = 1.   This is a specific case of the <111> zone axis. Let us examine a more physical example of the Weis's zone law that may help us tie a few of the concepts together. In figure 3.9 below we see another example from Silicon but this time the beam comes down the <110> zone axis.

---

[4] Higher order Laue zone effects in electron diffraction and their use in lattice parameter determination, P.M. Jones, G.M. Rackham, J.W. Steeds, Proc. R. Soc. London, A.354 pp 197-222 (1977)
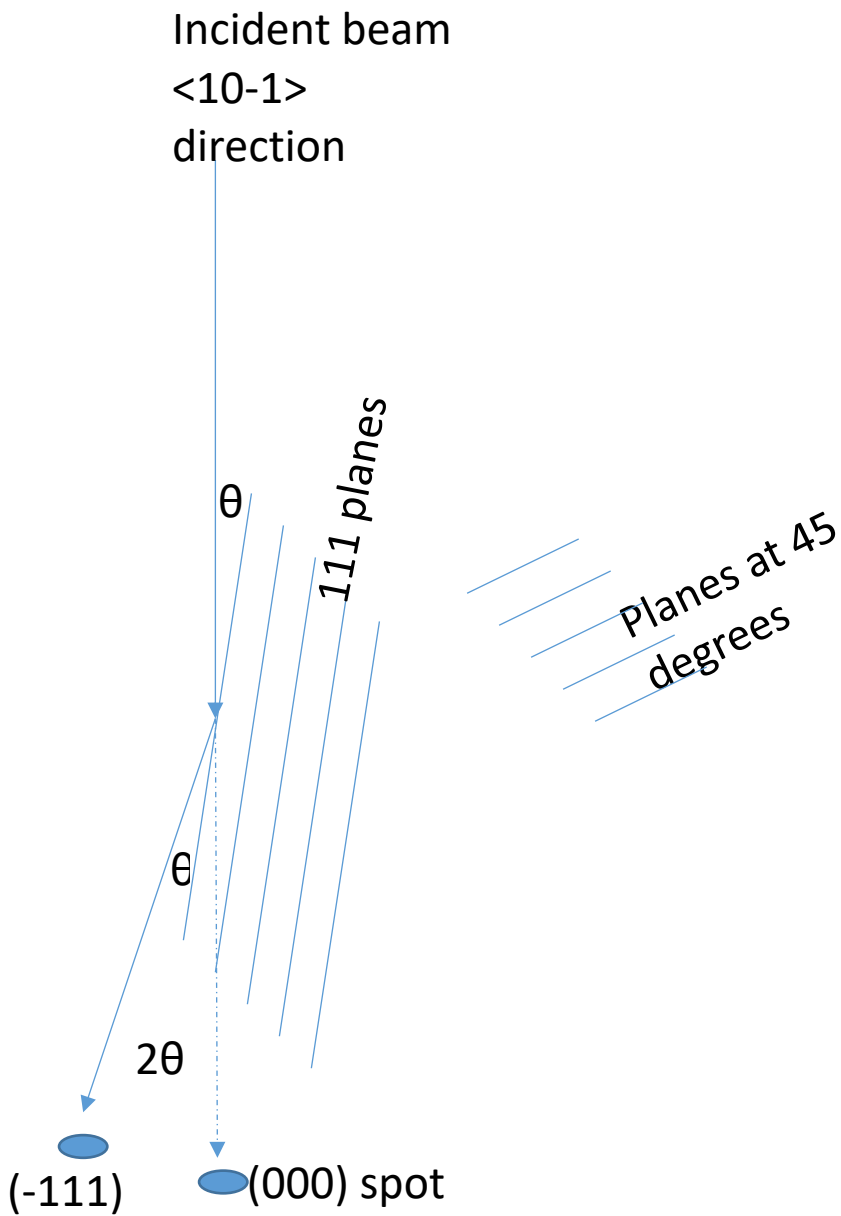
Incident beam
<10-1>
direction

θ

111 planes

Planes at 45
degrees

ɵ

2θ

(-111)

(000) spot

Figure 3.9 shows strong diffraction for beams parallel to the beam and offers a physical interpretation of Weis' zone law. To diffract, the Electric field that points perpendicular to the beam direction has to interact with dipoles in the material and this only can occur when the beam is parallel to the beam [5] Based upon this argument would you expect diffraction from the planes inclined at roughly 45 degrees?

---

[5] Dr. Greg Long, Hewlett Packard private communication.

As a hint, consider the planes to be roughly of 110 orientation and consider the Weis' zone law dot product.

Notation and brackets around Miller indices. In case you have not figured it out yet, (hkl) refer to planes, <hkl> is a direction, {hkl} is a family of planes such as {111} area all six planes (111), (**1**11), (1**1**1), (11**1**), (**11**1), and (**111**). Where boldface is a negative index such as **1** = -1. Similarly <110> is the family of directions that include [110], [**1**10], [1**1**0], [**11**0], [011], [01**1**], [0**1**1],[0**11**], [101], [**1**01], [10**1**], and [**101**]. A materials scientist is familiar with these 12 slip directions as they are the 12 slip directions of the close packed plane in an FCC material like Copper or Aluminum.

Let's use our fundamental's of reciprocal lattice we have learned so far to create an artificial diffraction pattern. We will keep it simple and consider the cubic P lattice. The P lattice is short for primitive and it has a lattice point at all 8 cube vertices as in figure 3.10.
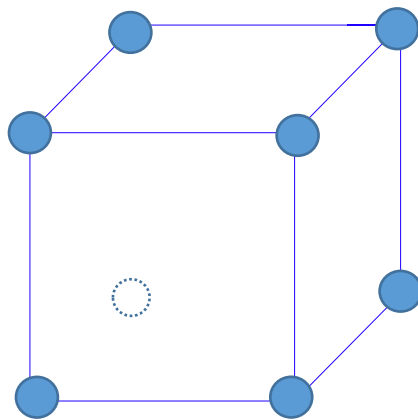

Figure 3.10 Primitive lattice with an atom at every cube vertices. The eight atom has dotted lines to show that it is hidden and provides perspective.

Let us consider the beam coming down the <110> direction of the crystal. From above we know the Miller indices are reciprocal lattice vectors, this is a cubic situation and so [110] direction of the crystal is the [110] direction in the reciprocal lattice and so from Weis's zone law we expect to see only (001), (**1**10), (1**1**1) planes. From our discussion of distance in the reciprocal lattice, we know that low indices will have the smallest distance from the origin. Thus (110) reflections will be root 2 further from the origin than the (001) refection. Let's draw these two reflectors, figure 3.11 below, at 90 degrees to each other as there dot product is zero.

000   001

$\dfrac{1}{a}$

$\dfrac{\sqrt{2}}{a}$

1-10

<110> directions in red

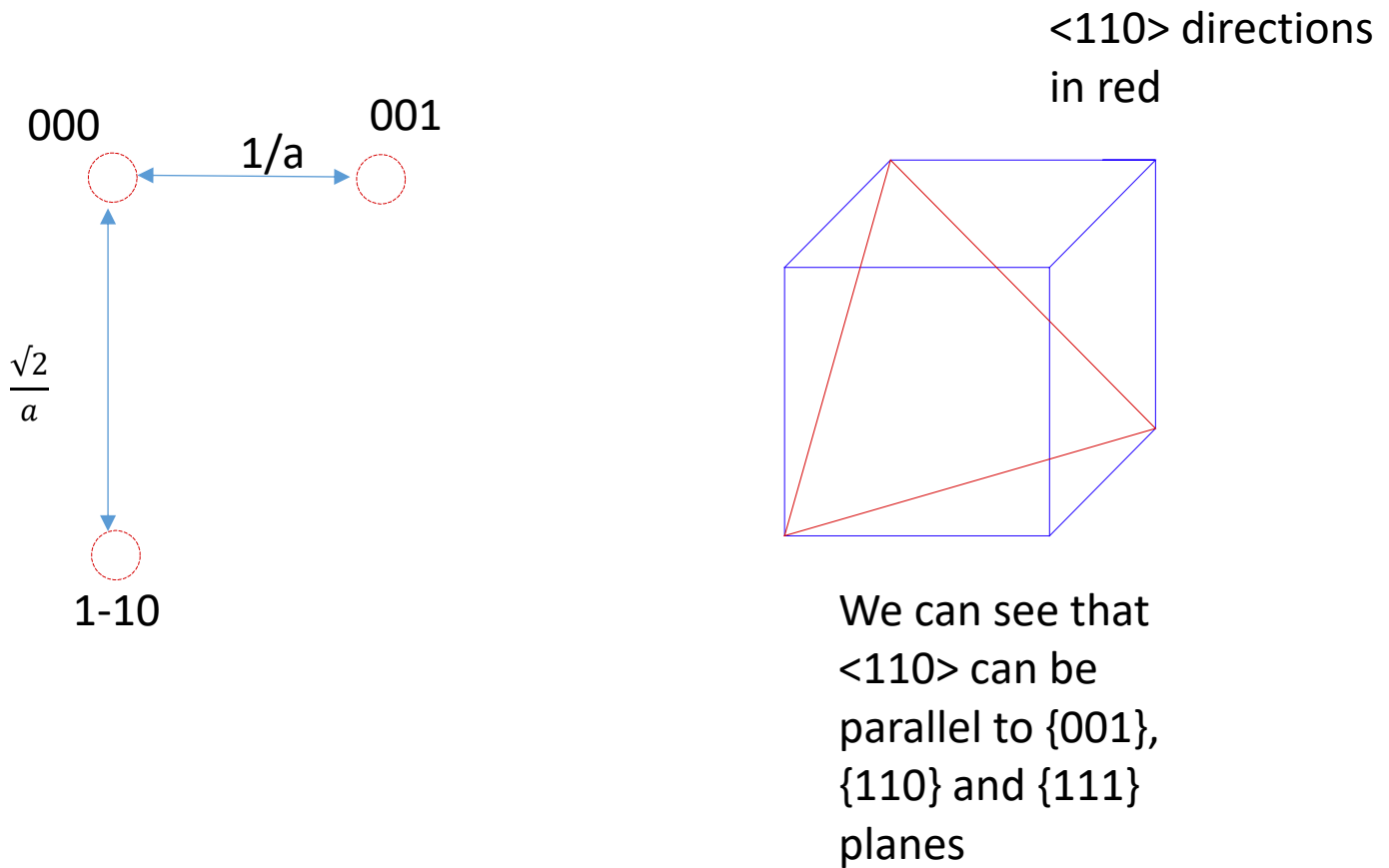We can see that <110> can be parallel to {001}, {110} and {111} planes

Figure 3.11 The reciprocal lattice points also known as diffraction pattern for primitive lattice with the beam coming down the [110] zone axis. The origin is marked 000 and corresponds to the non-diffracted original beam coming down the [110] zone axis.

the sum of the other points. [6] So we can create the 111 reflection that we also expect as the <110> family of directions are also parallel to {111} planes. We do this in figure 3.11 below.

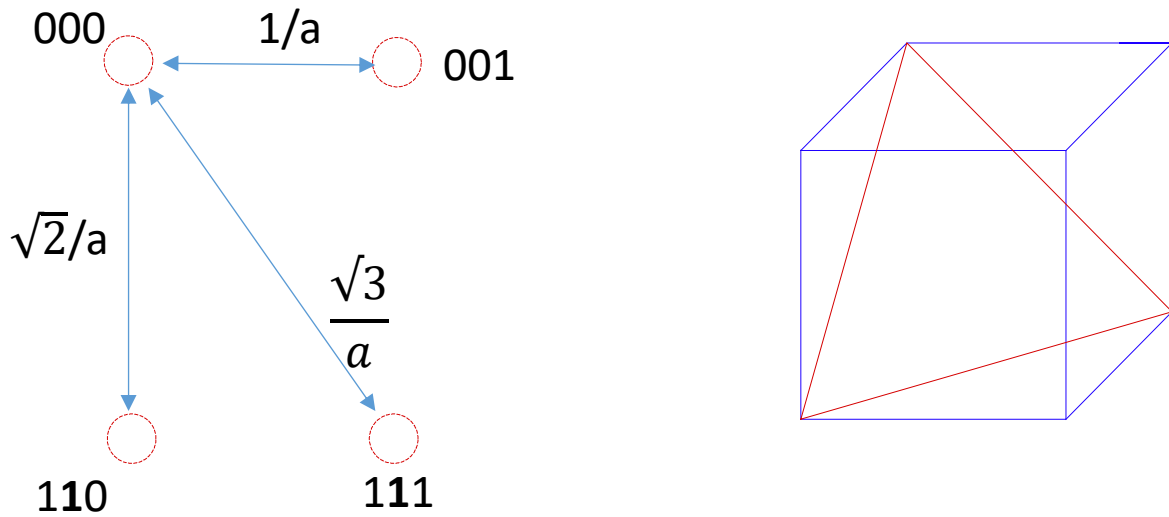[6] Bhadeshia, Crystallography course, Lecture 7 , online via www.openculture.com

Figure 3.12 The first three reflectors from [110] zone axis beam on a primitive cubic latest from first principles, ab initio. The real space lattice is at the right for reference. Bold face Miller indices are negative.

Now that we have the lower quadrant of the diffraction pattern we can easily visualize the symmetric reflectors such as -11-1 and 010. Or we can add other higher index reflectors by adding the first two reciprocal lattice vectors 1-10 to 001 to arrive at the desired reflector. Or in the words of linear algebra or modern physics, the 1-10 and 001 reciprocal lattice vectors form a basis for every known lattice reflection, point in reciprocal space. Real quick, how do we now find the inter planar spacing of say the {111} planes in this lattice? We simply take the inverse of the distance from the 1-11 to the origin in the figure or $a/\sqrt{3}$.

Now that we have covered the basics of how a diffraction pattern forms in a solid material we will explore a tool to visualize orientations and k space itself, the Stereographic projection. I admit that stereographic projections are hard for me but I will cover the basics then refer you to materials science texts like Reed – Hill and or TEM texts like Fultz and Howe chapter 7.   The stereographic projection is a method of understanding a three dimensional crystal on two-dimensional paper. Great circles will encircle all the active reflectors for a certain zone axis and the number of great circles will be the same as the number of symmetries. For example (100) planes will comprise 4 great circles, and (111) will have three great circles.   We will see the symmetry of the crystal immediately with the stereographic projection, without further delay let's start by constructing a stereographic projection, see figure 3.13.
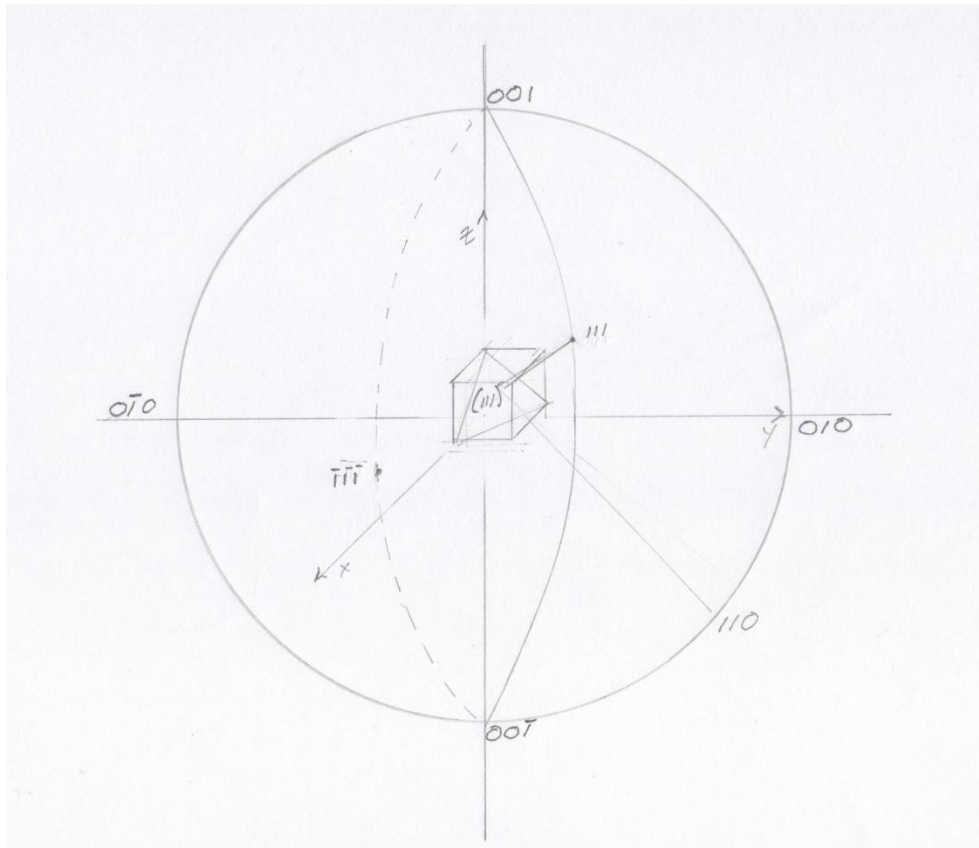
Figure 3.13 Step one of stereographic projection, draw the crystal in center and extend normal to major planes out to intersect sphere.

Step one of making a stereographic projection is to draw the crystal then extend the normal out to intersect the sphere. In step two we take draw projection lines from these intercepts to the south pole and record where they cross the equator.
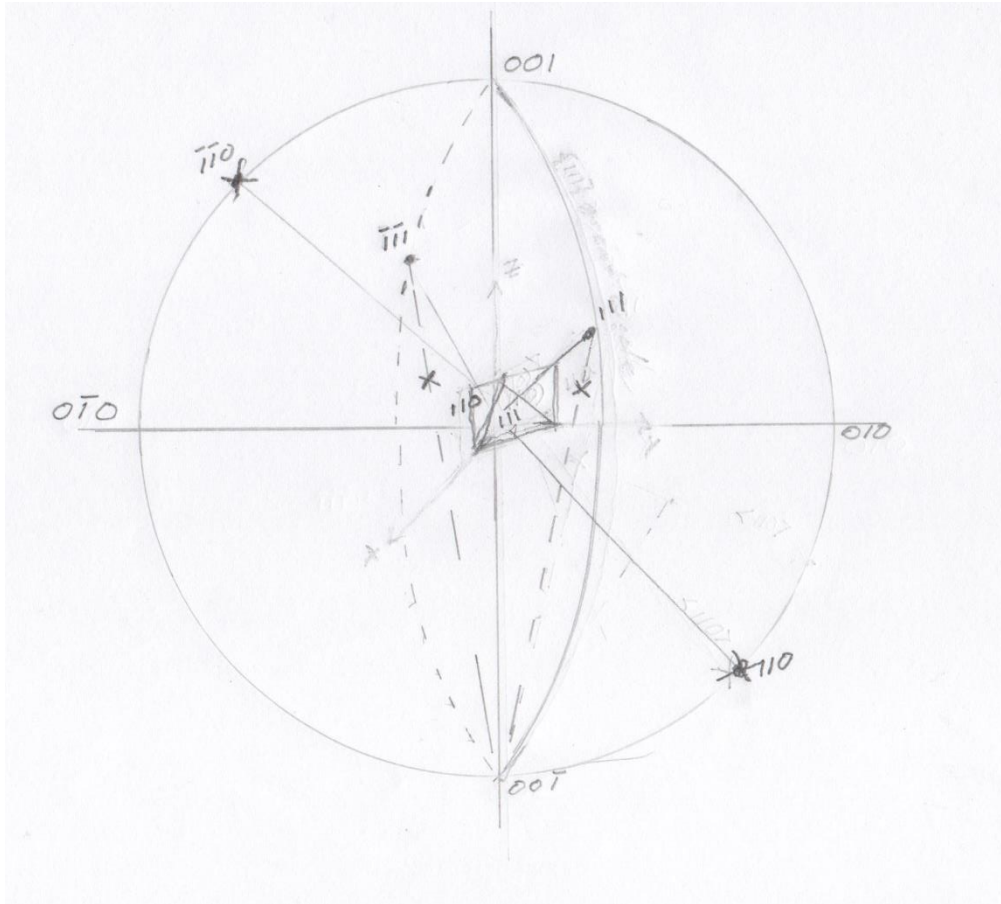
Figure 3.14 Step 2 of a stereographic projection from two planes as drawn, 110 plane and 111 plane. The normal to these two planes intersect the sphere. A projection of these planes to South Pole is done with dotted line and x marks where that projection crosses equatorial plane.

The two planes of the crystal in figure 3.14 give the two x spots. One on the equator edge at 110 and the other towards upper right at 111. Now we draw the equatorial plane to show these intersections more clearly, figure 3.15 below.
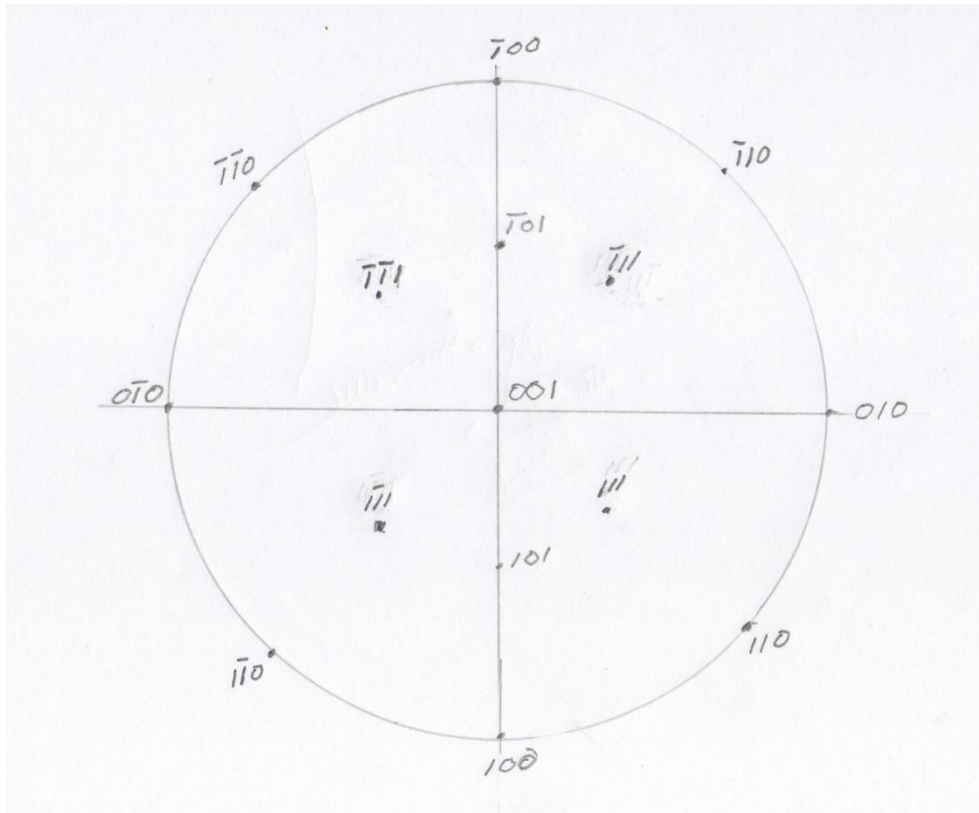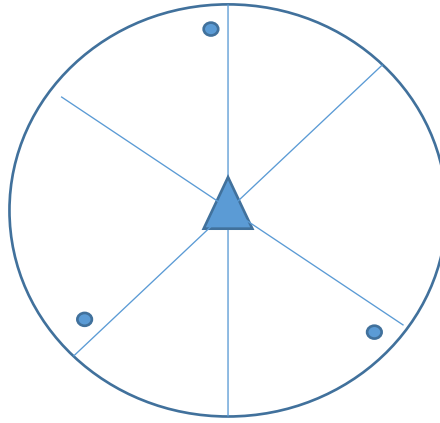
*Figure 3.15 Step 3 we draw where the projections cross the equator. Or we took the equator slice from the spheres of the two figures. Our 111, and 110 planes are shown in the lower right quadrant. It is always good practice to label the center (pole) of the projection, in this case the north pole, center of equatorial plane, is 001. Note 11-**1 is not labelled as it is below in the southern hemisphere.***

Looking at the stereographic projection you should note right away that relationships of distances between diffraction spots! Nor does the stereographic projection have information on structure factors, whether a scattering is allowed or not! For instance, in a diffraction pattern, the 111 reflectors would be much further away than the 100 reflectors but in the stereographic projection of figure 3.15 the {111} family is well inside the 100 and then close to the {101} family.   What is preserved in a stereographic projection? Or what good is it? The angles are preserved and can be measured by overlaying with a Wulf net, appendix 1.   Again, I will leave this to the materials science texts such as Reed Hill. Aside from these shortcomings, the stereographic projection is very good at representing the overall symmetry of the crystal.   And if the center, 001 is the zone axis then the great circle on the perimeter encompasses all of the planes that satisfy Weis's zone law and therefore may contribute to a diffraction spot, if the structure factor is satisfied. For example, in FCC 110 would not be allowed while in BCC 010 would not be allowed. Angles between the reflections on a great circle can easily be measured and a Wulf Net of the correct size to measure the angles of reflections in Figure 3.15 appears in Appendix A3.4.
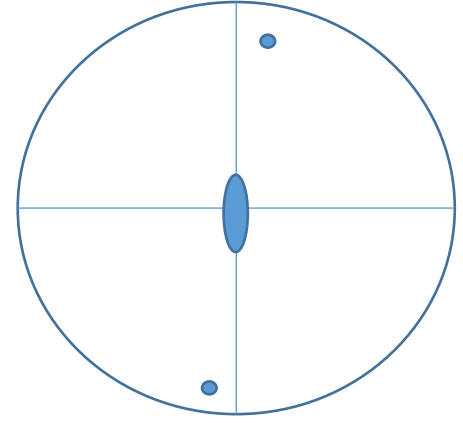
The stereographic projections can really help us visualize symmetries. For example the two fold rotational symmetry, 3 fold rotational symmetry and four fold rotational symmetry present in Cubic systems. These point group symmetry can be easily visualized in figure 3.16.
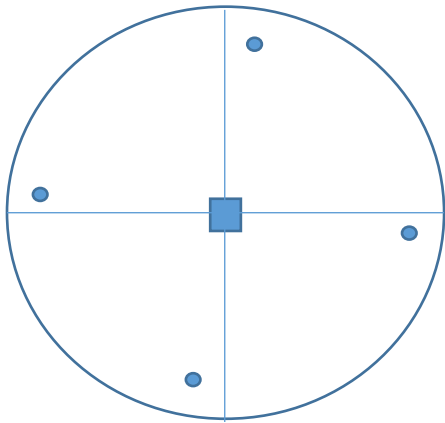
| Tetrads, 4 fold axis of rotation, six cube faces but 3 axis of symmetry, | Triads, 3 fold axis of rotation. 6 faces of 111 type or body diagonal. Or 3 of these axis., C_3 | Diads 2 fold axis of rotation 12 corners and 6 axis of symmetry, C_2 |

Figure 3.16 The rotational symmetry operations of a cube corresponding to a rotations through the faces, vertices, and edges. The corresponding symmetry operations are labelled as C4, C3 and C2. Note, to denote inversion symmetry in the stereogram, an open circle would be present. For example, C6h, discussed below would be 6 points every 60 degrees with an open and solid circle ontop of each other.

In figure 3.16 we have introduced our first symmetry operation, the rotation, Cn, where n is 4 ,3, 2 in the case illustrated. Some of the other symmetry operations that characterize a crystal are listed here but discussed in a later chapter: σ, reflection, σv reflection about a vertical axis, i for inversion, E for identity, and S for improper rotations. These groups of symmetry operations are lumped together as defining elements for the point group of which there are 32 cyrstallographic point groups. It should be mentioned that 11 of the point groups have i, inversion, as a symmetry element and are the so called centrosymmetric point groups and are the only ones uniquely determined by XRD. All 32 point groups can be determined with TEM electron diffraction, so as a microscopist, you have that to hang your hat on. In addition electron diffraction can also determine left and right handed or enantimorphism.

In figure 3.16 we mentioned the C_{6h} symmetry operation or the 6 fold rotation with a reflection about a horizontal plane. This stereogram is drawn below and will be our last discussion of symmetry operations until a later chapter. The C6h symmetry operation is illustrated below in figure 3.17.
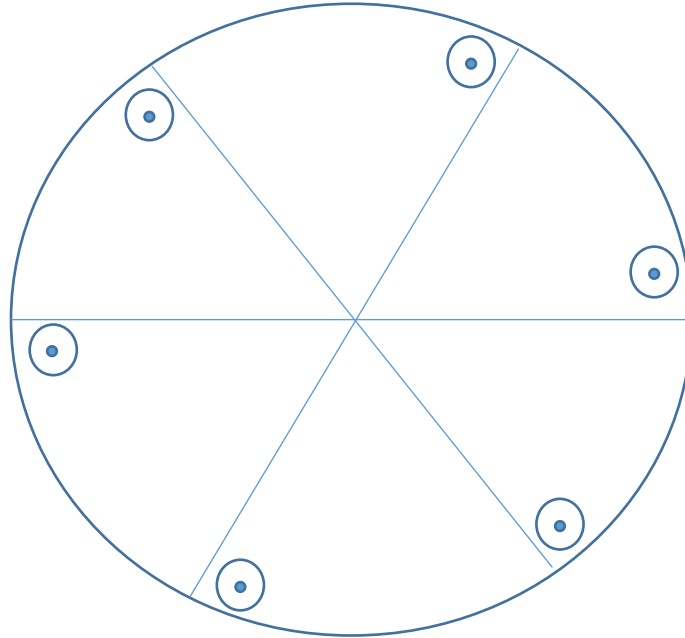
$$C_{6h} = C_6 * E * \sigma_h$$

Figure 3.17 The stereographic projection for the C6h point group comprised of the three successive symmetry operations that generate this point group.

The unfilled circles in Figure 3.17 represent the lattice points below or in the southern hemisphere. The solid circles inside the untilled circles are the projections from the Northern hemisphere. The fact that the solid points are inside the unfilled points means that this point group has perfect reflection symmetry about the horizontal plane. More examples of point groups will be given in a later chapter and the reader is referred to the excellent text by Burns. [7]

      A discussion of diffraction patterns would not be complete without touching on Kikuchi lines. Although Kikuchi lines are a symptom of a thicker sample we can use them to our advantage as a roadmap to the zone axis we need. Often when I make TEM samples with the focused ion beam, FIB, I leave one window thicker so that I am assured of getting Kikuchi lines so the sample can be oriented on a desired zone axis. An example of this is the [110] zone axis pattern for Silicon from the Oregon State University Titan TEM in figure 3.18 below.

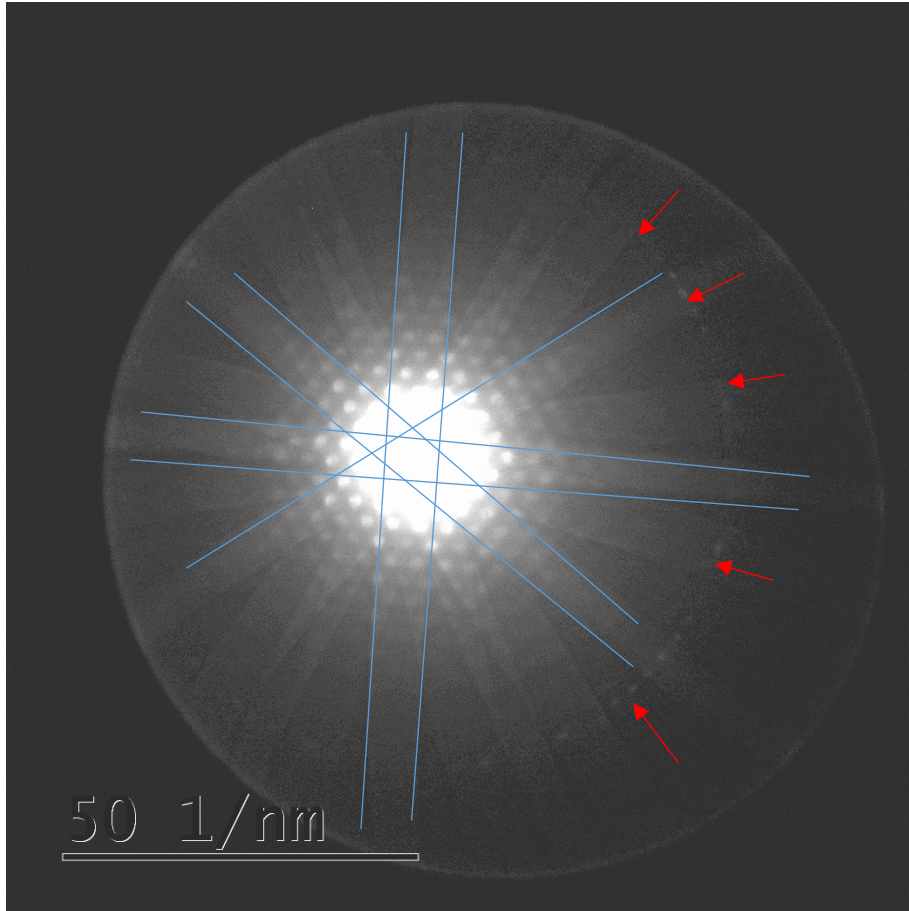[7] Gerald Burns, "Solid State Physics," Academic Press, Chapter 1, 1985.

Figure 3.18 Si in rough 110 orientation and corresponding cross of Kikuchi lines in blue. Also seen on the right side is the First order Laue Zone ring marked in red arrows.

The slightly offcenter pattern, due to not being able to re do it during Covid 19 shutdown shows the Kikuchi bands and the first order Laue Zone. The Kikuchi lines intersect at a zone axis, in this case the [110] zone axis. As we tilt the beam we look for the intersection of the Kikuchi lines to go towards the middle of the screen. We use alpha tilt to move the intersection (zone axis right and left) and beta tilt to move the zone axis up and down. Obviously, we needed to move this zone axis a bit more to the right with slightly more alpha tilt. Just as a note, the radius of the first Holz (Higher order Laue Zone) can be used to calculate the unit cell dimensions perpendicular to the beam. A more expanded pattern, larger camera length is then used to calculate the dimensions of lattice constant parallel to the beam using the zero order Laue zone spots.

We present a short discussion on how to draw your own Kikuchi bands given an indexed diffraction pattern. Using one of the indexed patterns in Williams and Carter or Fultz and Howe we draw a line from the pattern center to reflector hkl. Then we draw a perpendicular bisector to this line

and that is Kikuchi line hkl.   We continue on like this until we have a complete pattern, as shown in figure 3.19.
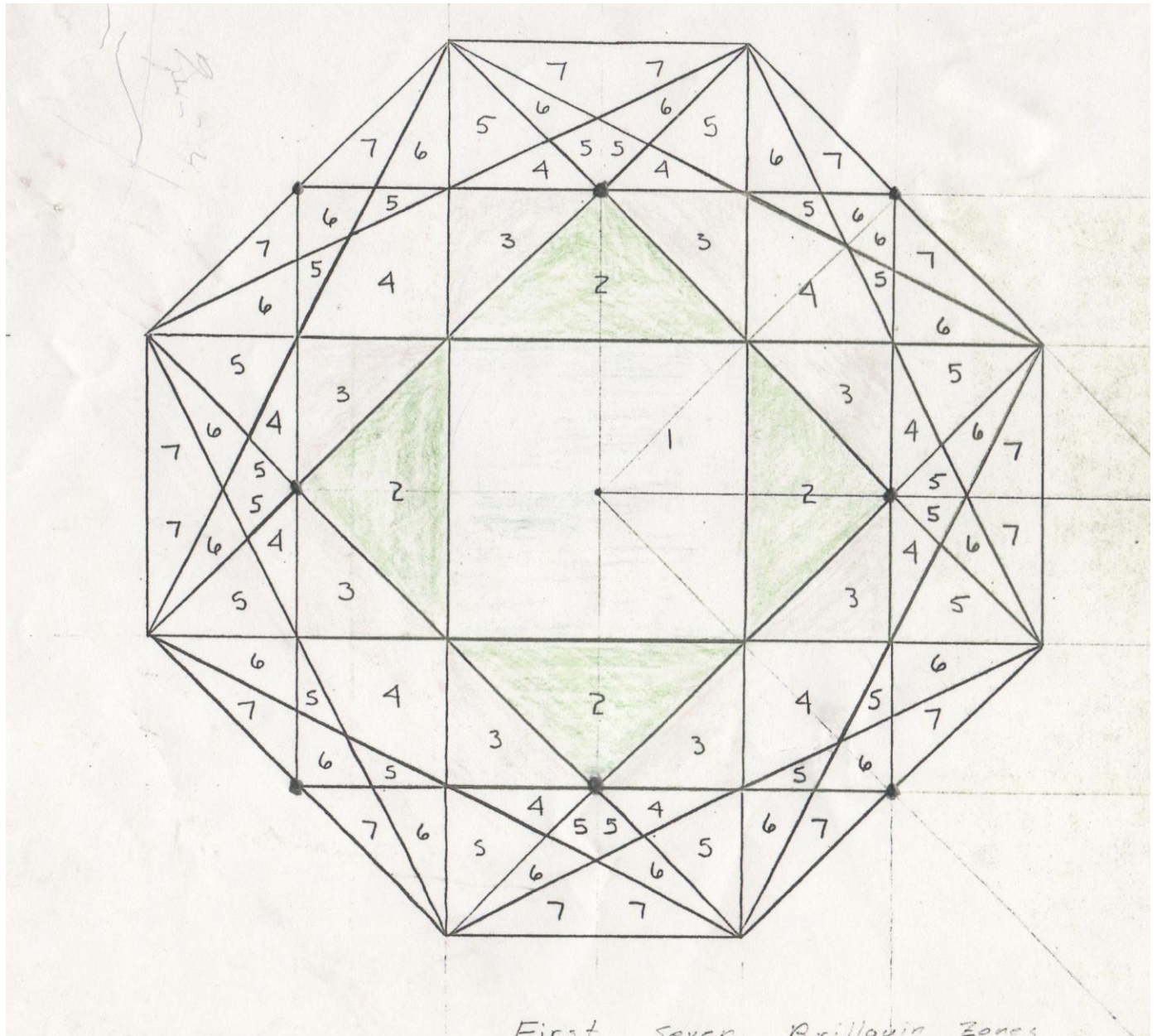

Figure 3.19 Frist Seven Brillouin Zones in a simple cubic reciprocal lattice. Brillouin zones have the same construction as Kikuchi lines as Brillouin zones are where the standing electron waves pile up to give the constructive interference of diffraction.

Figure 3.19 is from the Authors homework set in solid state Physics 563 at Washington State University, 1985. In that homework, a reciprocal lattice was bisected into Briillouin zones.   The construction is the same as that of Kikuchi lines. And note from the definition earlier of reciprocal lattice page 2: a1* = $\frac{a2^{\wedge}a3}{a1 \cdot a2^{\wedge}a3}$, a2* = $\frac{a3^{\wedge}a1}{a2 \cdot a3^{\wedge}a1}$, and a3* = $\frac{a1^{\wedge}a2}{a3 \cdot a1^{\wedge}a2}$, the reciprocal lattice is also cubic!

Actual TEM samples have a disk shape to them and the disk has a thickness, so the Ewald sphere constructions of earlier figures in this chapter need to be modified for real world samples. The idealized lattice needs to be convolved with the FT of the sample disk. The resultant are "relrods" or ellipses in reciprocal lattice space as follows in figure 3.20.

Lattice

Sample

FT of Lattice

FT of sample

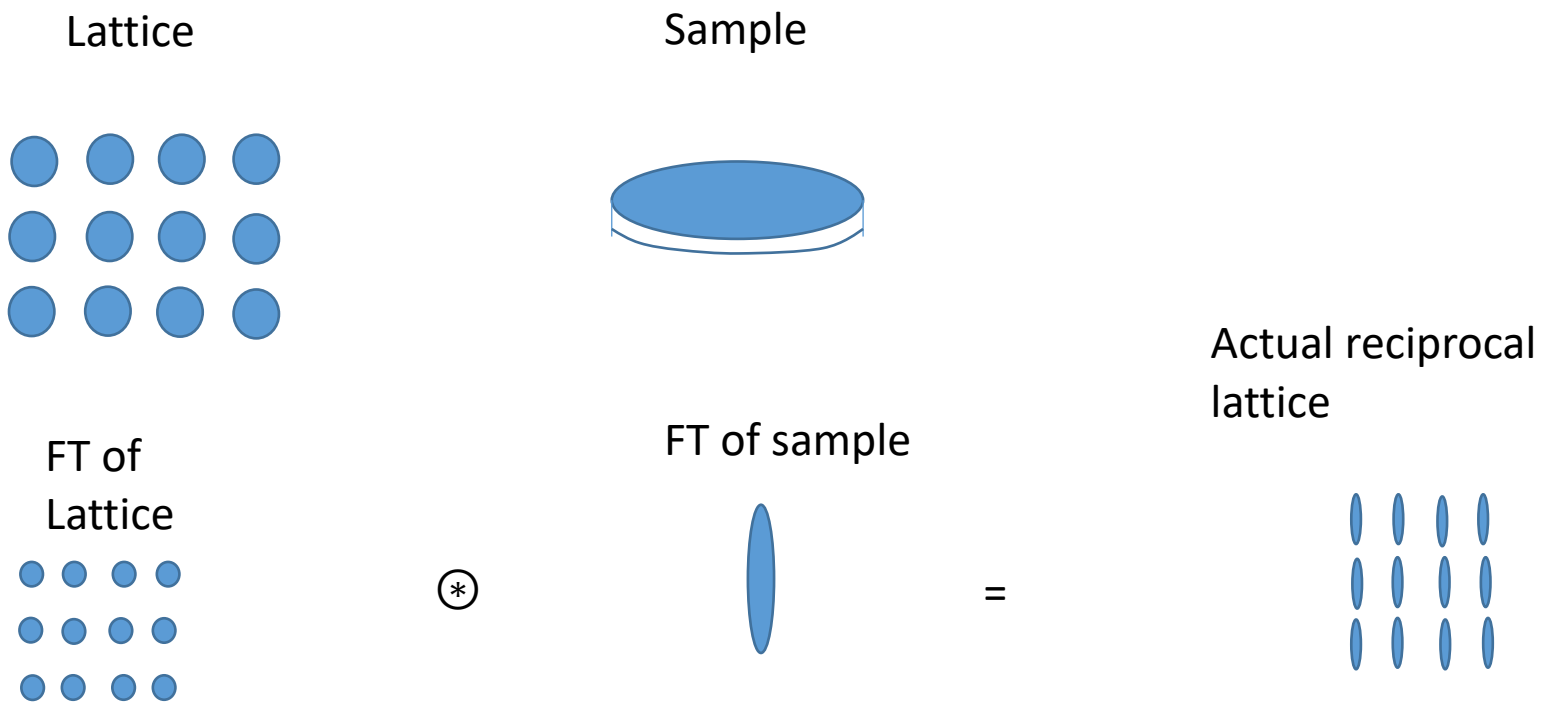Actual reciprocal lattice

$*$

$=$

Figure 3.20 The effect of sample shape on reciprocal lattice. The former points of reciprocal lattice become relrods.

So, now, the diffraction becomes easier to obtain. This elongation is one aspect of electron diffraction that is a plus and a minus. On the plus side, it does allow for more planes to satisfy the diffraction

condition. On the minus side, it makes for less accurate measurements. There are some tricks to enhance the accuracy, always, if you can, measure the –g to g distance in a diffraction patern and divide by two. This will be covered in a paragraph to follow. For now, lets examine how the relrods affect the number of planes we see, figure 3.21 below.
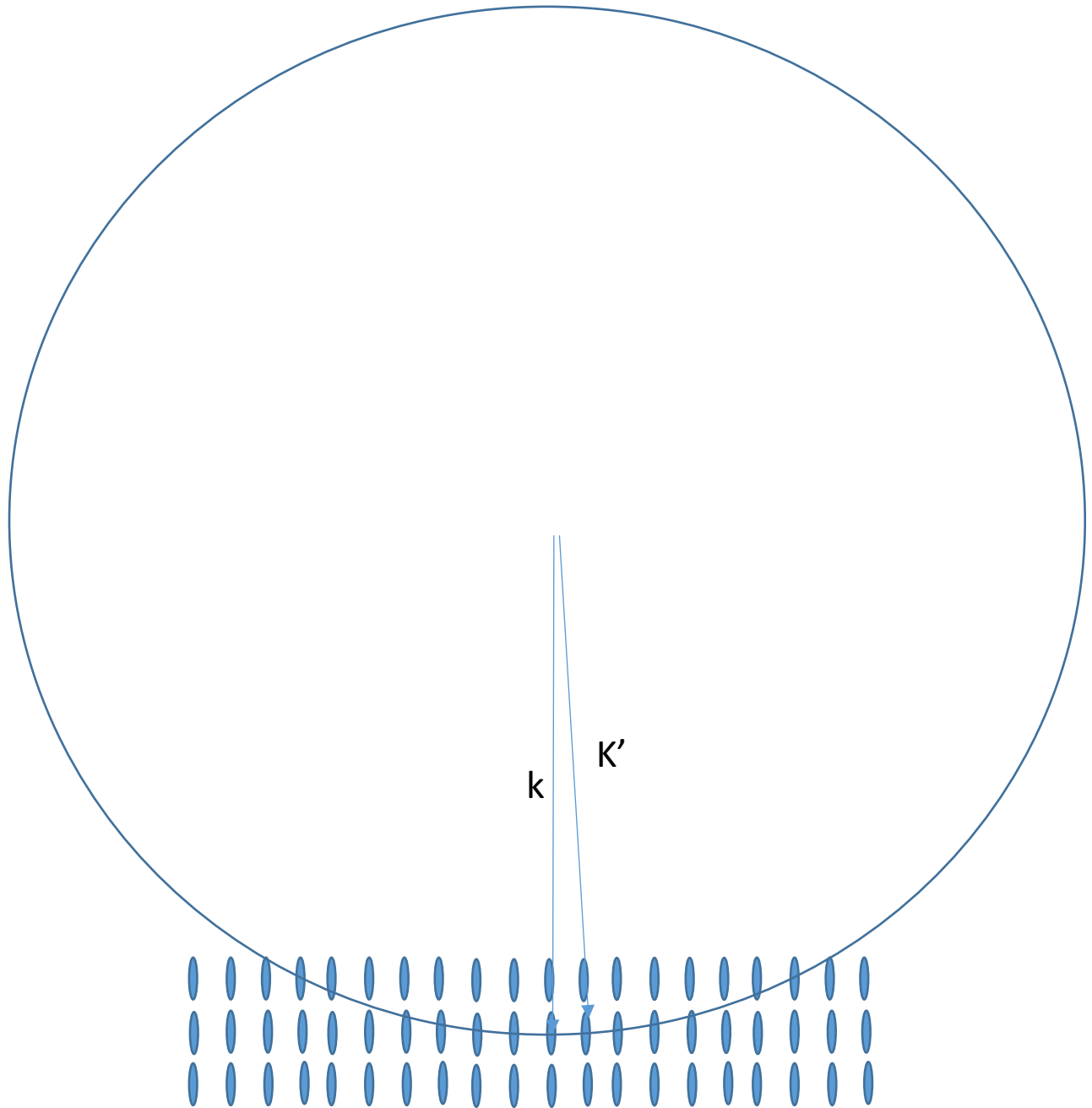

Figure 3.21 Our real world Ewald construction with a thick disk sample and the associated relrods. We can see the Ewald Sphere intersects a lot more reciprocal lattice relrods giving us more diffraction spots (planes) in our pattern.

The relrods of the figure above show that many more reflectors are going to be present in an electron diffraction pattern than we might have previously thought. One other practical aspect of relrods is that the ellipses may not go up and down as they do in figure 3.21. What happens if we observe a crystal that is thin in one direction but tilted to another zone axis not in the thin direction? This can also happen in precipitates of hcp in an FCC material and is discussed in detail in Fultz and Howe. [8] An example showing the non vertical relrods (reciprocal lattice rods) and the problems they cause for use is shown in figure 3.22 below.
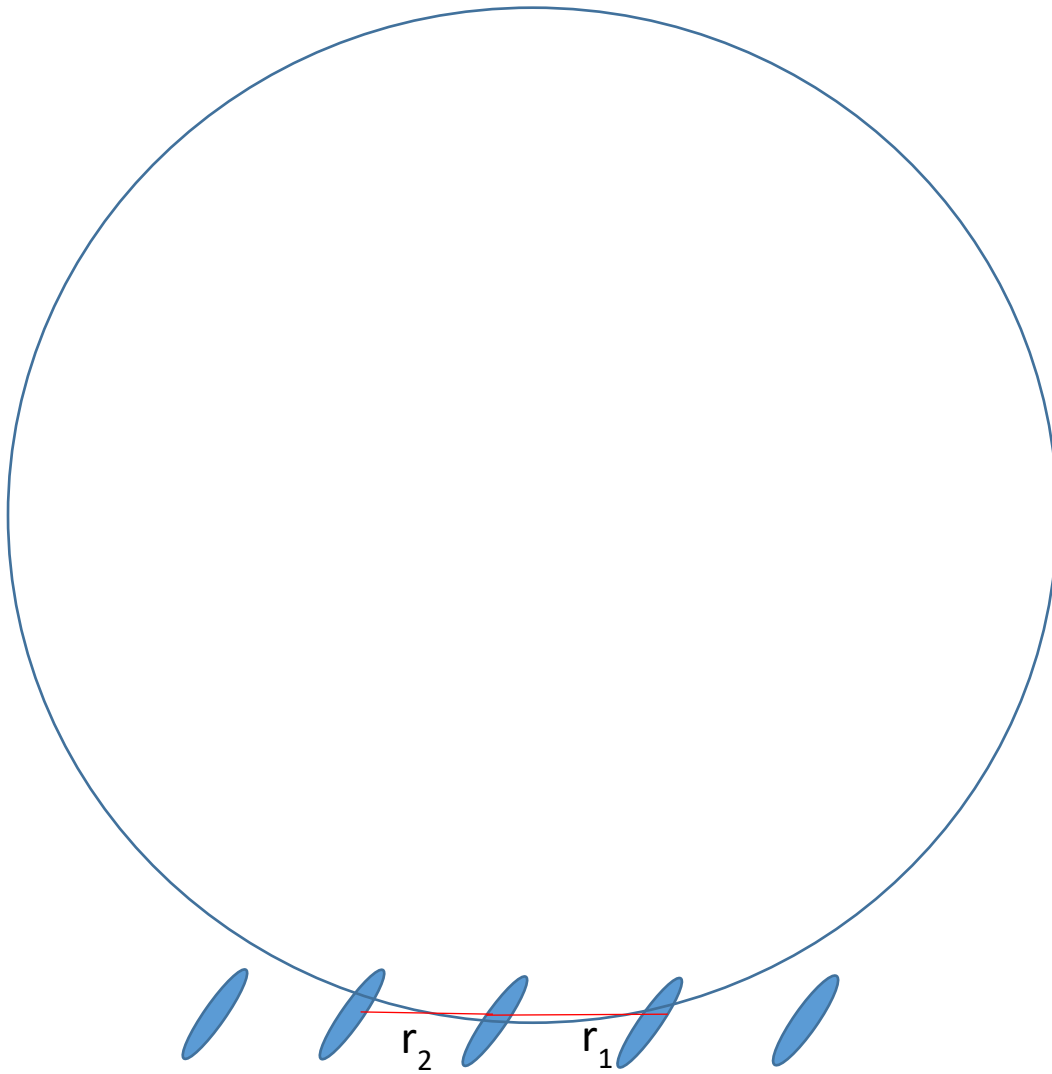
Figure 3.22 Shape factor convolved with lattice points for long platelets or precipitates that do not line up with zone axis of the base crystal. The shape factor results in an r1 > r2.

In the figure above we see the effect on measurements of lattice spacing can be fairly large and for this reason we are better served by measuring the distance between two spots and dividing by 2 to average

[8] Transmission Electron Microscopy and Diffractometry of Materials Vol 4, Fultz and Howe, Springer, pp 280-281.

out shape factor distortion like this. Diffraction Tools, a freeware plugin for the Digital Micrograph software has a provision for center to point measurement or the preferred point-to-point measurement (where it takes care of dividing by two and inverting the reciprocal lattice distance to real distance in nanometers. Examples using Digital Micrograph are presented in the Appendix.

Complex patterns around bright central spots are sometimes seen in alloys or multiphase materials. Some of these shapes are due to the case of "superlattice" reflections – breaking of excluded reflectors by chemical substitution in the lattice and others are due to a secondary phase. We will now discuss both of these. The terminology of "superlattice" is not familiar to all of the materials scientists that I have encountered.   For years I was calling attention to some weak reflectors in a student's sample and saying they were evidence of a super lattice. This assistant professor kept sending the student back to look for a "secondary phase." Finally, I realized that what the assistant professor was calling a secondary phase was actually the "superlattice" reflections that we had observed long ago. Or we were talking about the same phenomenon but using a different language.

The first type of complex diffraction pattern of weaker spots around a brighter central spot is truly due to the shape factor, or relrod effect, from elongated crystallites of a second phase growing into a primary phase but in specific directions. This is the case with aluminum – silver alloys where streaks of thin hexagonal close packed phase(HCP) lie along four {111} directions in an underlying face centered cubic (fcc) phase. [9] In the case of these thin disks of HCP manifest themselves as a pattern that looks like a four leaf clover or a child's jack from the game of jacks, using Fultz and Howe's analogy.
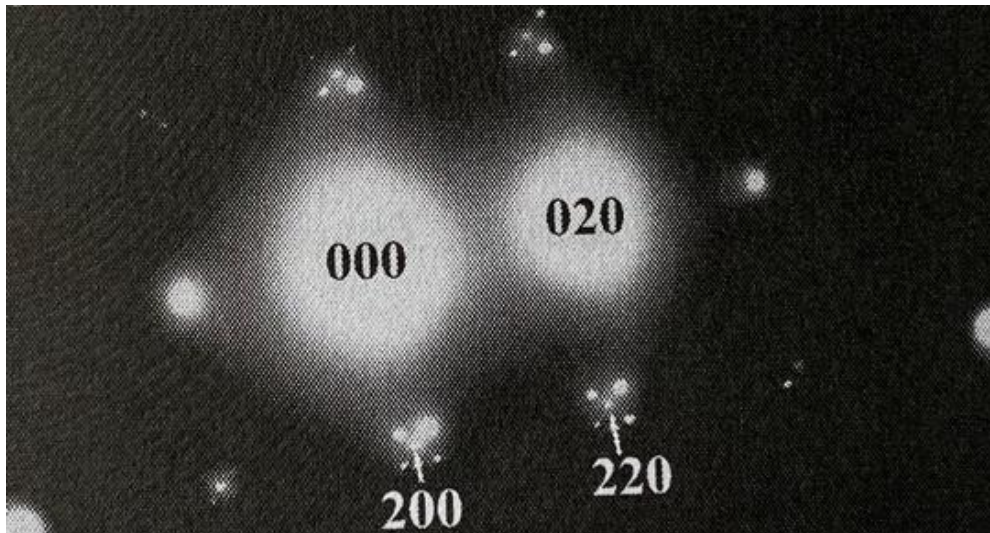

Figure 3.23 [001] Zone axis pattern from an FCC Al-Ag alloy with hcp gamma' precipitates showing the Jack pattern as the gamma' phase aligns to all four (111) planes.

---

[9] Fultz and Howe, "Transmission Electron Microscopy and Diffractometry of Materials," 4th Edition, 2013. Springer, Figures 6.27 and 6.26.

A second very common observation of weaker patterns around bright spots in engineering is due to "chemically sensitive," diffractions. These are diffractions such as {100} in BCC patterns. The (100) reflections cancel pairwise (Fultz and Howe pp 253-254) but if the atoms at the corners are different pairwise cancellation is broken. This is discussed as the Strukturbericht (German, structure report) B2 phase in Fultz and Howe. [10] The B2 phase or CsCl phase allows the {100} reflectors! In metal alloys these {100} reflectors show up as reflectors at half the spacing of the more common {200} BCC reflections. In an alloy these {100} reflections can be quite weak depending upon how much alloying agent is present or quite strong in an intermetallic where the alloying agent is appreciable. An example Strukturbericht pattern is shown below in figure 3.24.
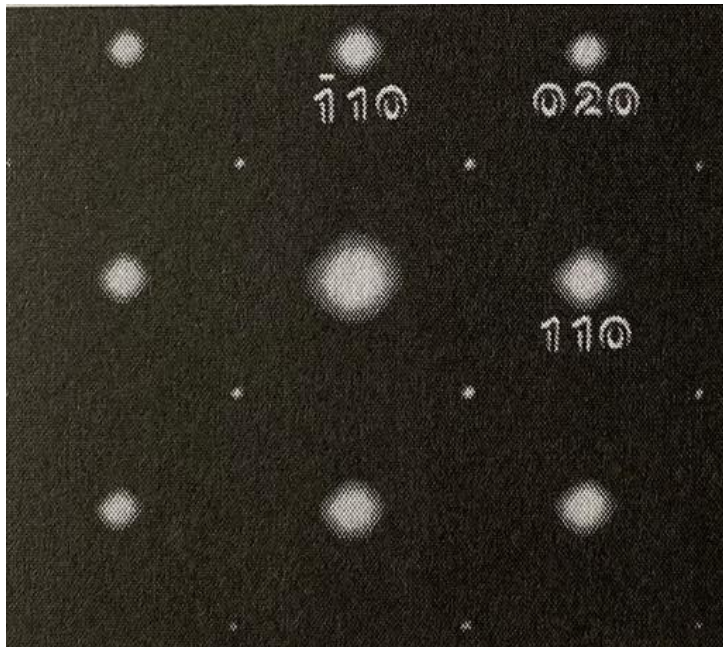

Figure 3.24 Strukturbericht B2 pattern of Ti Based alloy with 4 weak diffraction spots at half the spacing of the 020 reflectors showing that the {100} reflections are now allowed. A pure BCC metal would have none of these reflectors as the (100) and ((1/2,1/2, ½) reflections cancel pairwise due to the $\frac{\pi}{2}$ phase shift between them. From Fultz and Howe, figure 6.10.

A third type of complex diffraction pattern is due to the super lattices of the type we study in electronic properties of materials. Namely, layered structures such as multiple layers of Ge-Si

---

[10] Ibid, pp 258-259

heterojunction solar cells, GaAs – AlGaAs light emitting diode structures.   If the layers are thin and periodic we will see fine points that blur the diffraction pattern in the direction of the layers.

A fourth very advanced pattern is double diffraction from two phases. In double diffraction, there are second set of reflectors that have lattice constants that differ by the difference of the two lattice constants and these patterns can be very difficult to interpret. I am looking for examples of double diffraction, so if you have one please let me know and will happily add it to this discussion. Double diffraction can be a real test of your geometry skills.

Diffraction relies heavily on our ability to visualize geometrical patterns.   To help with that we have discussed plane geometry, the Miller Indices, the Ewald sphere construction as an alternative to Bragg's diffraction law, remember k – k' = g? The stereographic projection was also introduced as a way to visualize and measure angles in a diffraction pattern, although to be honest I simply form the dot product between to zone axis that I want and compute the angle directly.   However, for some the stereographic projection is helpful. If your struggle with it, as I do, you can be a diffraction success without it. Relrods or shape factors from the convolution of sample shape and diffraction relax diffraction conditions.   Finally, more advanced diffraction phenomenon like secondary phases, superlattice or Strukturbericht patterns were introduced. Diffraction is a whole discipline to itself and every day I learn something new, keep an open mind and keep learning.


Appendix, Indexing patterns.

For this example the sample is single crystal silicon.

1. Measure spot spacings to create a table of d spacings.
   a. Choose 4-6 spots to start with.
   b. For better accuracy, measure the largest distance possible (N multiples) symmetrically across the transmitted spot, then divide by N.
   c. d-spacing is the inverse of the measured distance to the diffracted spot ($\hat{g}$).

2. Compare the list of d-spacings to potential matching solutions by searching ICDD.

*Si is a very close match, though, the measured $\hat{g}_1$ (2.715 Å) does not appear in the PDF card data. At this point, it would be better to just ignore this, revisiting it later. When the structure is determined (diamond cubic), structure factors may reveal this is a forbidden spot (but appears here due to double diffraction effects). The next systematic spot further out happens to be the 400 spot, which is not forbidden, and matches the measured spacing well (2.715/2).

Table 1: Si d-spacings from ICDD.

Silicon PDF Card #00-005-0065

2 Theta	d (Å)	I	h	k	l
28.419	3.138	100	1	1	1
47.3049	1.92	60	2	2	0
56.1019	1.638	35	3	1	1
69.1709	1.357	8	4	0	0
76.3699	1.246	13	3	3	1
88.0561	1.1083	17	4	2	2
94.9716	1.045	9	5	1	1
106.7311	0.9599	5	4	4	0
114.1258	0.9178 ·	11	5	3	1
127.568	0.8586	9	6	2	0
136.925	0.8281	5	5	3	3
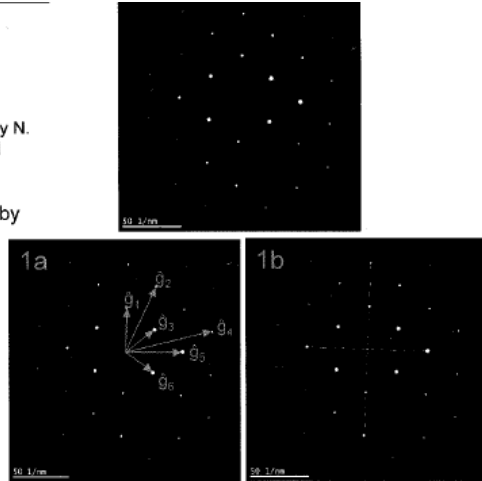
2. Compare Real to Measured d-spacings

Table 2: Measured d-spacings .

Spot	M = Measured Value (1/nm)	N = Multiples of distance to g measured	d = 1/(M/N) Units: nm	d (Å)
g1	14.734	4	0.2715	2.715
g2	12.224	2	0.1636	1.636
g3	19.108	6	0.3140	3.140
g4	15.984	2	0.1251	1.251
g5	10.403	2	0.1923	1.923
g6	19.009	6	0.3156	3.156

1a 1b

Slide #23

Figure A3.1 JEOL, Japan Electron Optics Laboratory inc., guide to indexing page 1. This guide is very useful; it is rumored to have been written by an Intel Engineer and passed onto JEOL. Measure your prominent spacings then compare with those in ICDD.

Comparing Table 2 in figure A3.1 with Table 1 we see that g3 is probably the {111} family of planes while g2 is probably the {311} family, and finally g5 is likely the {220} reflector. All of the distances are given in the ICDD, international center for diffraction data, database, which we do have in the electron microscope facility at OSU. We should always pause for a second and think about selection rules or structure factors from our Fourier representation. Diamond cubic, which is the Si structure, is two FCC lattices one displaced from the other by ¼,1/4,1/4. As such the indices should be all odd or all even (FCC structure factor). That is true. And in addition, there is no reflection for which h + k+ l = 2n, where n is odd. Eg, h + k + l = 2, h + k +l = 6 , …. Are not allowed. This is also true.

A quick discussion on calibration of the TEM in diffraction mode is due and will now be discussed. Back in the day, TEM's were not as easy to calibrate as they had film cameras. And the first discussion of an older school TEM person was to teach you about camera length and how to calibrate your photographs. This is decidedly old school and will not be taught here! Now it is quite easy to calibrate a TEM camera in diffraction mode. If the EM facility has done its job the TEM will be calibrated to +- 2 percent on all camera lengths (magnifications in diffraction mode). If you do encounter a diffraction pattern with spacings that do not make sense then please do the following: 1) let me know and I will recheck the calibrations at the camera lengths and lens conditions that you used, and 2) compute ratios of your distances and compare with ratios of known reflectors in the data base. You can

often index an un-calibrated TEM in this manner as the ratio of distances cancels out the unknown camera length (magnification factor).

Now we move onto step 3,4, and 5 of indexing, guessing at reflectors and zone axis verification. This is the most difficult portion of our job indexing a pattern.

DIFF – Indexing an Electron Diffraction Pattern (SAD)

*For this example the sample is single crystal silicon.

3. Identify the diffracted spots.
   a. Begin by labeling general hkl's to individual spots, (direct from the PDF card; for $\hat{g}_5$, d=1.92Å, hkl = 220).
   b. These general hkl labels now need to be adjusted (by guessing) to fit the laws of vector addition.
   *In this example, $\hat{g}_3 + \hat{g}_6 = \hat{g}_5$ must be true but <111>+<111>≠<220>, so these indices are not correct. However, if $\hat{g}_3$ or $\hat{g}_6$ were <11-1>, which is still in the same family of planes, this would work. So, arbitrarily we choose to change one of them, $\hat{g}_6$, and continue testing. Also, $\hat{g}_3 + \hat{g}_5 = \hat{g}_4$ must be true and <111>+<220>=<331>. So these indices appear to be correct, so far.
   c. These hkl assignments now need to be tested against the angles between them using the dot product rule.
   *The angle θ, between $\hat{g}_5$ and $\hat{g}_6$, measures 84.7 degrees. The following equation must be true:
   $\cos \theta = (h_1h_2 + k_1k_2 + l_1l_2)/ |\hat{g}_5| |\hat{g}_6|$
   It is true in this case.
   Measure and test other angles for more verification.

4. Repeat these measurements and verification on 1-2 other zone axes.

5. The beam direction <UVW> is the zone axis direction. To determine this compute the cross-product (vector) of any two indexed spots on the pattern.
   In this example: $\hat{g}_5 \times \hat{g}_6 = (-220)$
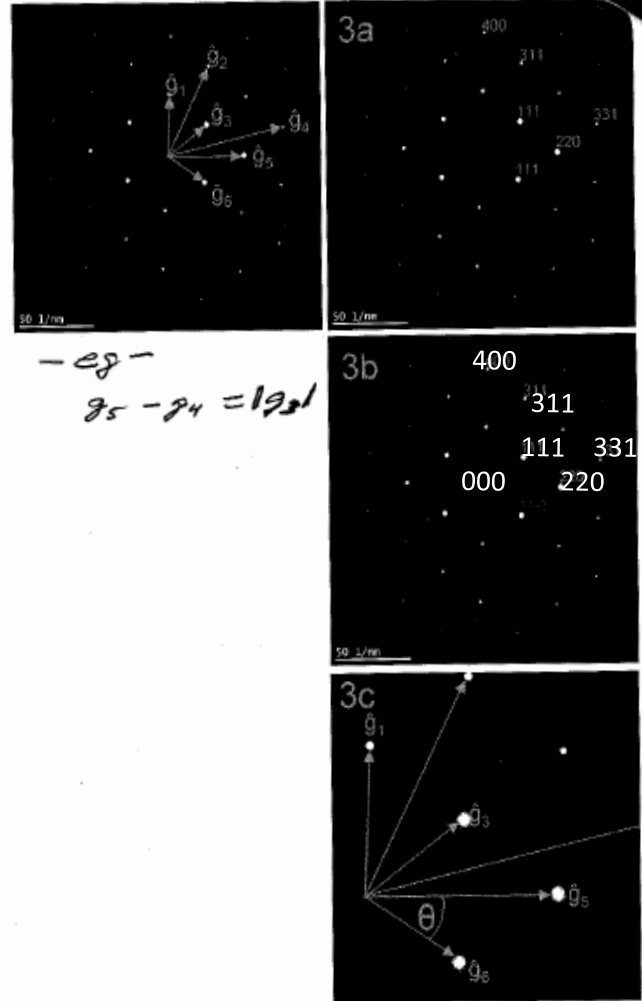

Figure A3.2 Steps 3, 4, 5 we guess the indexing and then verify by checking vector addition, and that any reciprocal lattice point is a sum of others.

From step 3 above we notice that 400 is allowed for Si but 200 is not and yet g1 should be 200. Realize that the sample was probably thick and so double diffraction (111 +1-1-1 for example, or 111 scattering went on and then scattered from a nearby 1-1-1 plane) occurred yielding a 200 spot. So, g1 is assigned 200. G2 is assigned at 311. G3 is assigned as 111. G4 is assigned 331. G5 is assigned 220. Finally, g6 we guess is 11-1. We then verify our g6 assignment by checking to see if g6 + g3 = g5, and it does. So, we

guessed correctly on g6. Now let's try other additions, from inspection of the above we should have g3 + g1 = g2,

 and g3 + g1 = 111 +200 = 311 that is our guess for g2. So, far so good.   Let's finally check the last triangle of vectors, g3 + g5 = g4? Remember we add vectors head to tail so g3 slides over to the tail of g5 make the last leg of triangle. And checking this vector addition,

g3 + g5 = 111 + 220 = 331. Since g4 does equal 331. We have the final check, g3 + g5 = g4.   We are done with the indexing of this pattern.   Finally, some useful vector properties appear below.   They will be useful in the paragraph that follows where we verify angles.

Useful Rules for Vector Algebra

Vector Addition:
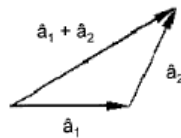
For two vectors $\hat{a} = (h_1 k_1 l_1)$ and $b = (h_2 k_2 l_2)$,
$\hat{a}_1 + \hat{a}_2 = (h_1 + h_2,\ k_1 + k_2,\ l_1 + l_2)$

Dot Products:
$$\hat{a}_1 \cdot \hat{a}_2 = |\hat{a}_1|\,|\hat{a}_2|\cos\theta = h_1 h_2 + k_1 k_2 + l_1 l_2$$

$$|\hat{a}1| = \text{sqrt}\,(h_1{}^2 + k_1{}^2 + l_1{}^2)$$

Angle test for index verification:
$$\cos\theta = (h_1 h_2 + k_1 k_2 + l_1 l_2)/\,|\hat{a}_1|\,|\hat{a}_2|$$

Cross Product:
$$\hat{a}_1 \times \hat{a}_2 = |\hat{a}_1|\,|\hat{a}_2|\sin\theta \quad \text{(scalar)}$$

Also, for a vector result,
$$\hat{a}_1 \times \hat{a}_2 = (k_1 l_2 - l_1 k_2)\,\mathbf{i} - (h_1 l_2 - l_1 h_2)\,\mathbf{j} + (h_1 k_2 - k_1 h_2)\,\mathbf{k} = (k_1 l_2 - l_1 k_2,\ h_1 l_2 - l_1 h_2,\ h_1 k_2 - k_1 h_2)$$

Slide #25

Figure A3.3 Vector properties and useful identities. My hand scribble appears and is my pneumonic for the cross product as a determinant.

We will do a more difficult example next using a student sample. In this case the student, from U of Oregon, came to OSU for indexing some samples that were Titanium dioxide. But there are two phases of Titanium dioxide, Anatase and Rutile. So, which one did she have? After collecting the patterns we set about to characterize them and those thoughts are presented here.
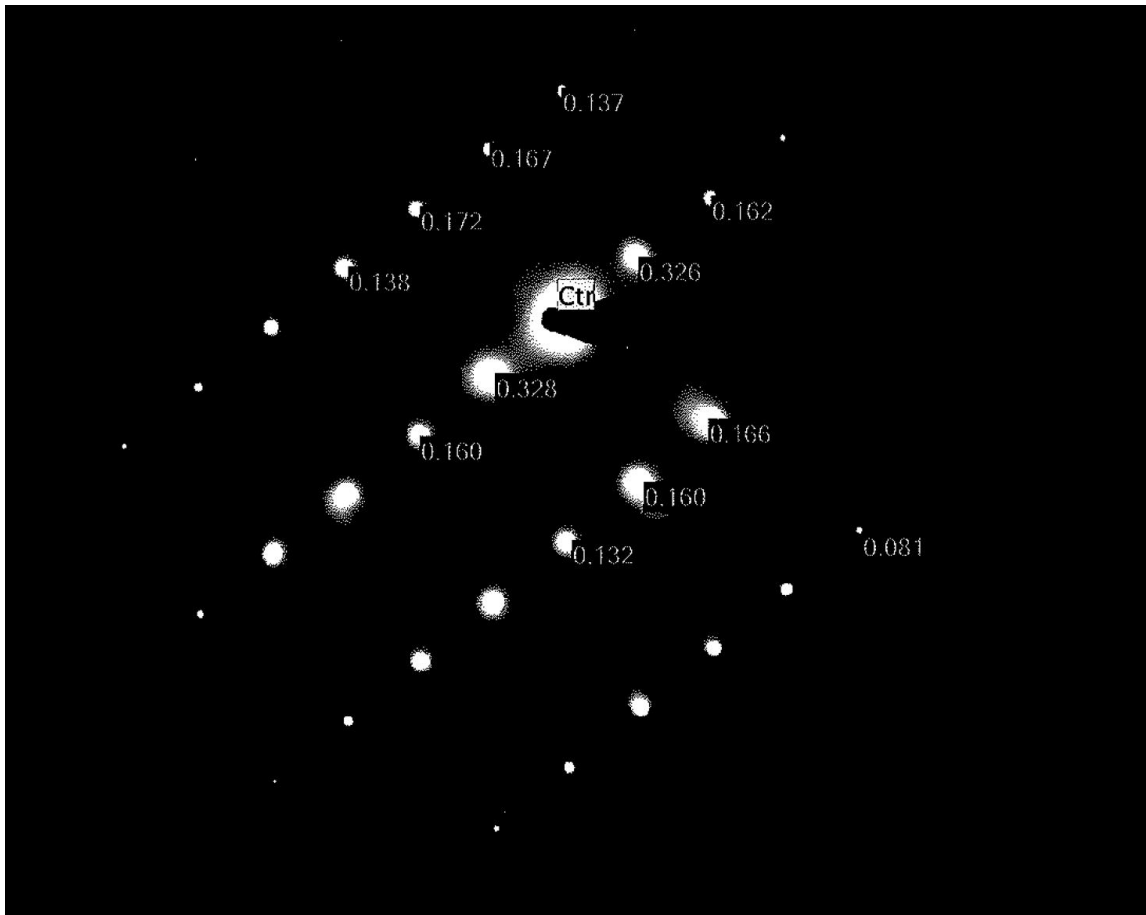

Figure A3.4 The near zone axis pattern for a crystallite of a mineral thought to be a phase of Titania. Marissa Acosta, University of Oregon. The distances, nm, were measured using the free "Digital micrograph: plug-in called Diffraction tools.

Next we write down all of the distances and how many there were and compare with distances from the International Center for Diffraction Data base (ICDD).

Jems comparisons:

1) Has Anatase <3,1,0?> symetry but <310>
   distances don't match

2) Anatase <311> has .3516 nm + .243 +.2352
   reflections for other sample!

3) Anatase <5X17>   .3516 * 2   .170 x 2   .15 x 2
                                                need 4!
4) Rutile <2X1>   .23 * 2   .134 .134x4

5) Rutile <113>   .325 x 2   .169 x 4   .162x2 .136x4

Figure A3.5 The diffraction peaks were jotted down along with the number of them. Anatase distances did not match observed.

Once the diffraction peaks were determined, we started comparing the distances from the known distances found in JEMS or the ICDD software. Note, that there are errors in the JEMS database and to save embarrassment, I would stick with the ICDD. However, later, JEMS can be used and was used to simulate the pattern as the JEMS simulation tools are superior. Rutile <113> was selected as a candidate and now have to go through and reconcile that with Figure A3.6 below from the ICDD database.
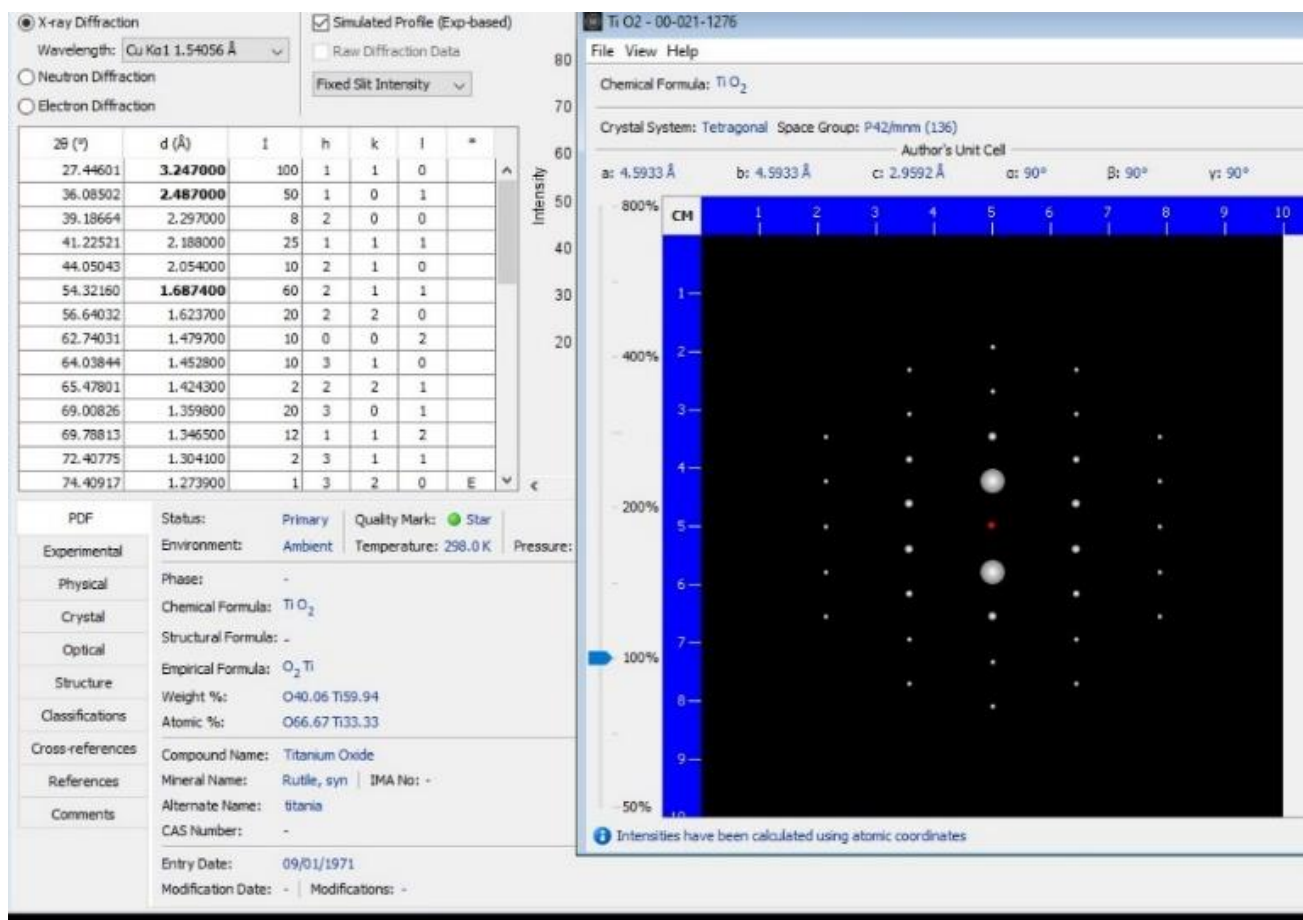
Figure A3.6 The ICDD database output. Two of the three major reflectors, in bold are an exact match to the database. Tetragonal phase space group 136.

Note the absence of 101 reflectors, 2.48 nm, why is this absent. To index this pattern we consider Weis' zone law ant that a proposed zone axis has to be perpendicular to the observed reflectors. To determine a zone, I cheated and scrolled through the patterns in JEMS until I found a Rutile pattern that matched the symmetry of the observed pattern of figure A 3.4. The match was for zone axis <113>. There is no way to make a dot product of <113> and (101) that vanishes. For example we can choose the (-1 1 0), as the .324 nm reflector and the (1-1 0) as the other and both vanish when dotted into <113>. But, we can not change the sign on the (101) family of reflectors to make the dot with the proposed <113> zone axis vanish! So, (101) is excluded from being observed in the <113> zone axis. What about the .168 nm reflectors, the proposed 211, if we choose (-2,-1 1) that dot product with <113> vanishes. We see that (21-1) also vanishes. Now we are left to explain the other two .165 nm

reflectors and find those by realizing that in the tetragonal system we can permute the h, k as those have the same distance. Therefore, the other two reflectors are (1 2-1) and (-1-2 1). Now we have all four .168 nm reflectors that vanish when dotted into <113>.   We are confident but now further check by looking further down the list, we also see four .136 nm reflectors we observed quite readily in the pattern. Those are the (0 3-1), (-301), (30-1), and (0 3-1).   We notice all four of these vanish when dotted into <113> as well.   We see the final indexed rutile simulation from JEMS with indices in figure A 3.7 below.

Figure A 3.7 JEMS simulation of Rutile in <113> zone axis. With the pattern indexed consistent with Weis' zone law and the distances measured

Angles should also be checked and can print them pattern and measure them with a protractor or we use the "Crystal tools plugin" in Digital Micrograph to obtain angles. This is particularly important in the non-cubic lattices such as Monoclinic, Triclinic.
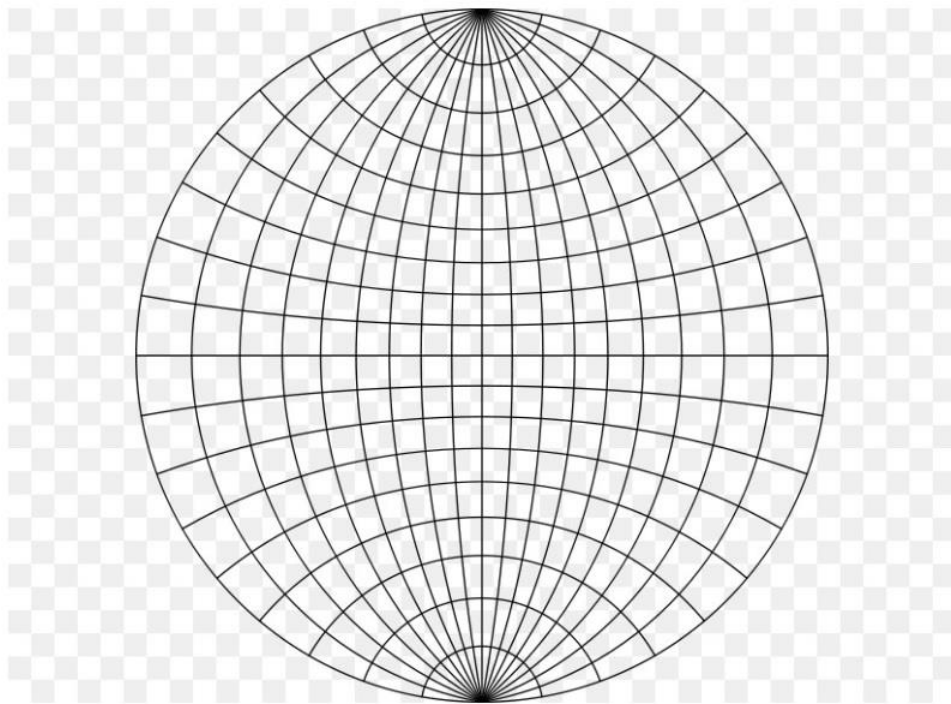
Figure A.3.8 Wulff Net of approximate size to measure angles on stereographic projections in this chapter

.